

Review

Graphene Utilization for Efficient Energy Storage and Potential Applications: Challenges and Future Implementations

Umair Yaqub Qazi ^{1,2,*}  and Rahat Javaid ^{3,*} 

¹ Department of Chemistry, College of Science, University of Hafr Al Batin, P.O. Box 1803, Hafr Al Batin 39524, Saudi Arabia

² Division of Nanomaterials and Chemistry, Hefei National Laboratory for Physical Sciences at Microscale, University of Science and Technology of China, Hefei 230026, China

³ Fukushima Renewable Energy Institute, National Institute of Advanced Industrial Science and Technology (AIST), 2-2-9 Machiikedai, Koriyama 963-0298, Fukushima, Japan

* Correspondence: umairqazi@uhb.edu.sa or umair@ustc.edu.cn (U.Y.Q.); rahat.javaid@aist.go.jp (R.J.)

Abstract: Allotropes of carbon are responsible for discovering the three significant carbon-based compounds, fullerene, carbon nanotubes, and graphene. Over the last few decades, groundbreaking graphene with the finest two-dimensional atomic structure has emerged as the driving force behind new research and development because of its remarkable mechanical, electrical, thermal, and optical functionalities with high surface area. Synthesis of graphene oxide (GO) and reduced graphene oxide (rGO) has resulted in numerous applications that previously had not been possible, incorporating sensing and adsorbent properties. Our study covers the most prevalent synthetic methods for making these graphene derivatives and how these methods impact the material's main features. In particular, it emphasizes the application to water purification, CO₂ capture, biomedical, potential energy storage, and conversion applications. Finally, we look at the future of sustainable utilization, its applications, and the challenges which must be solved for efficient application of graphene at large scales. Graphene-based derivative implementations, obstacles, and prospects for further research and development are also examined in this review paper.

Keywords: graphene; graphene derivatives; potential applications; challenges; energy storage



Citation: Qazi, U.Y.; Javaid, R. Graphene Utilization for Efficient Energy Storage and Potential Applications: Challenges and Future Implementations. *Energies* **2023**, *16*, 2927. <https://doi.org/10.3390/en16062927>

Academic Editor: Cai Shen

Received: 6 February 2023

Revised: 10 March 2023

Accepted: 17 March 2023

Published: 22 March 2023



Copyright: © 2023 by the authors. Licensee MDPI, Basel, Switzerland. This article is an open access article distributed under the terms and conditions of the Creative Commons Attribution (CC BY) license (<https://creativecommons.org/licenses/by/4.0/>).

1. Introduction

In the years after its first discovery by Prof Andre Geim and Prof Kostya Novoselov (200) at The University of Manchester who won the Nobel prize for physics [1], graphene has been one of the most talked-about subjects in materials science, prompting an abundance of research articles on its impressive physicochemical properties. This network of atoms is depicted in Figure 1 as a hexagonal structure [2]. Two-dimensional (2D) graphene is a honeycomb-structured sheet of carbon atoms. Several desired features, including strong mechanical toughness, electrical and thermal conductivity, and other astonishing characteristics, have been found in this material. For these reasons, many investigative attempts have been made to integrate graphene with polymers to create nanocomposite materials [3,4]. Owing to its complicated bottom-up production, low solubility, and aggregation in solution because of Van der Waals interactions, the utilization of pure graphene has been challenging to accomplish [5,6]. Reducing the amount of oxygen groups produces reduced graphene oxide which has more similar properties to pristine graphene such as higher solubility and higher reactivity as compared to graphene oxide. When graphite is oxidized in acidic solutions, graphite oxide is formed, consisting of several tightly packed layers of graphene oxide (GO) [7].

The hexagonal carbon structure of GO is comparable to that of graphene, which is embroidered with oxygen functionalities such as alkoxy (C–O–C), hydroxyl (OH), and carbonyl (C=O) functional groups [8]. Since no GO compounds occur naturally, the produced

“molecule” is non-stoichiometric. In practice, graphite is first oxidized to produce graphite oxide, which is then exfoliated to generate GO; it follows a generic primary chemical equation, as described here.

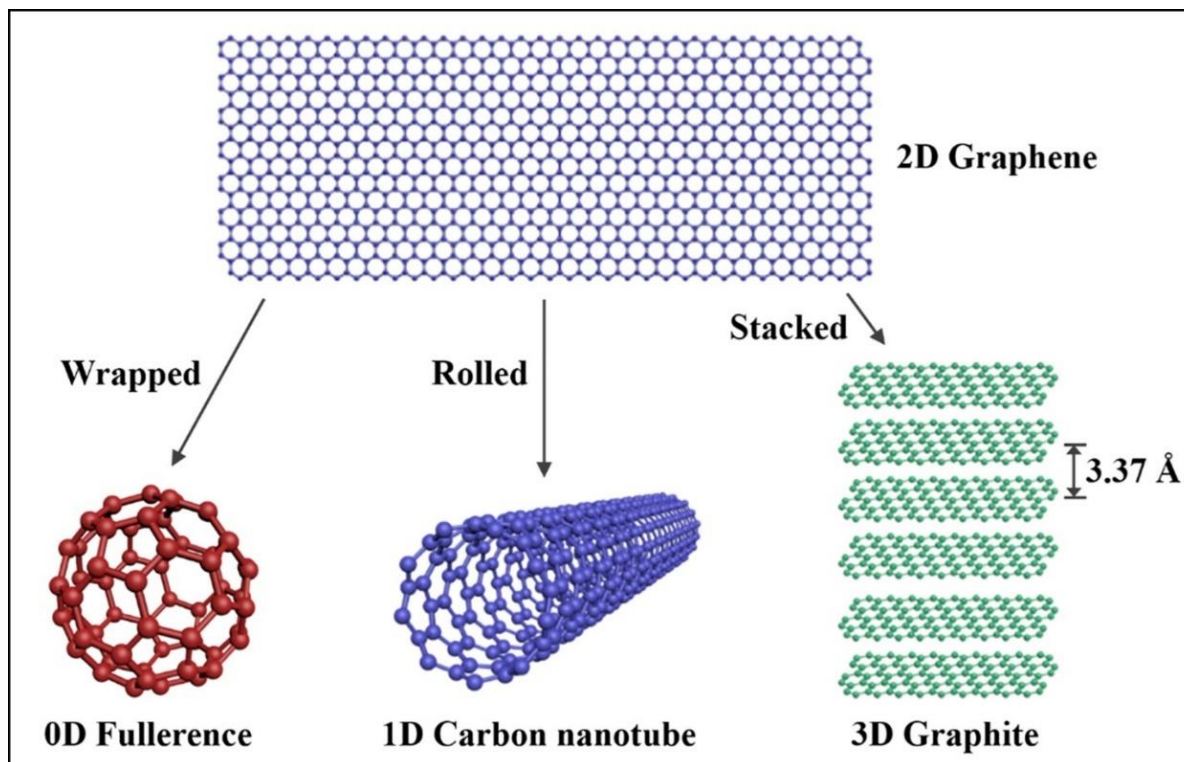


Figure 1. Allotropic forms of carbon structures. Reprinted with permission from Ref. [2].

Layers of carbon (Graphite) → Oxidation → Graphene oxide

Numerous advantages over the material are attributable to the existence of these oxygenated groups and the simplicity with which graphene can be synthesized. These advantages include increased solubility, greater flexibility [9], and the ability of surface functionalization, which has opened up many possibilities for utilization in nanocomposite materials. In an effort to reduce the number of oxygen groups and acquire properties more similar to those of pristine graphene, GO can be processed by a variety of ways to synthesize reduced graphene oxide (rGO) [10].

Graphene derivatives have been widely used as nanofillers in polymer nanostructured membranes because of their improved dispersibility and material characteristics in polymer matrices [11–13]. This has resulted in numerous developments in a wide range of scientific disciplines. The compact stacking of sp^2 hybridized carbon atoms is documented to work as a pretty close effective gas barrier molecule [14], showing its application in materials for packaging [15], Si-based NIR tunneling heterojunction photodetector [16], dual-enhanced photodetectors combining graphene plasmonic nano resonators [17], shielding for responsive electronic equipment [18], and indeed protective components against corrosive environment [19]. Due to the same driving factors, the perfect tune of filler stuff in nanocomposites may be utilized to change the electrocatalytic activity of specific-sized molecules to produce improved membrane technology [20]. The physicochemical, thermoelectric, and electroconductive characteristics of GO are also valuable for a wide range of other applications [20]. Figure 2 illustrates the structures of graphene and its derivatives [21]. Based on unique qualities and demands, numerous forms of graphene materials and derivatives stimulate their implementation in specific priority sectors.

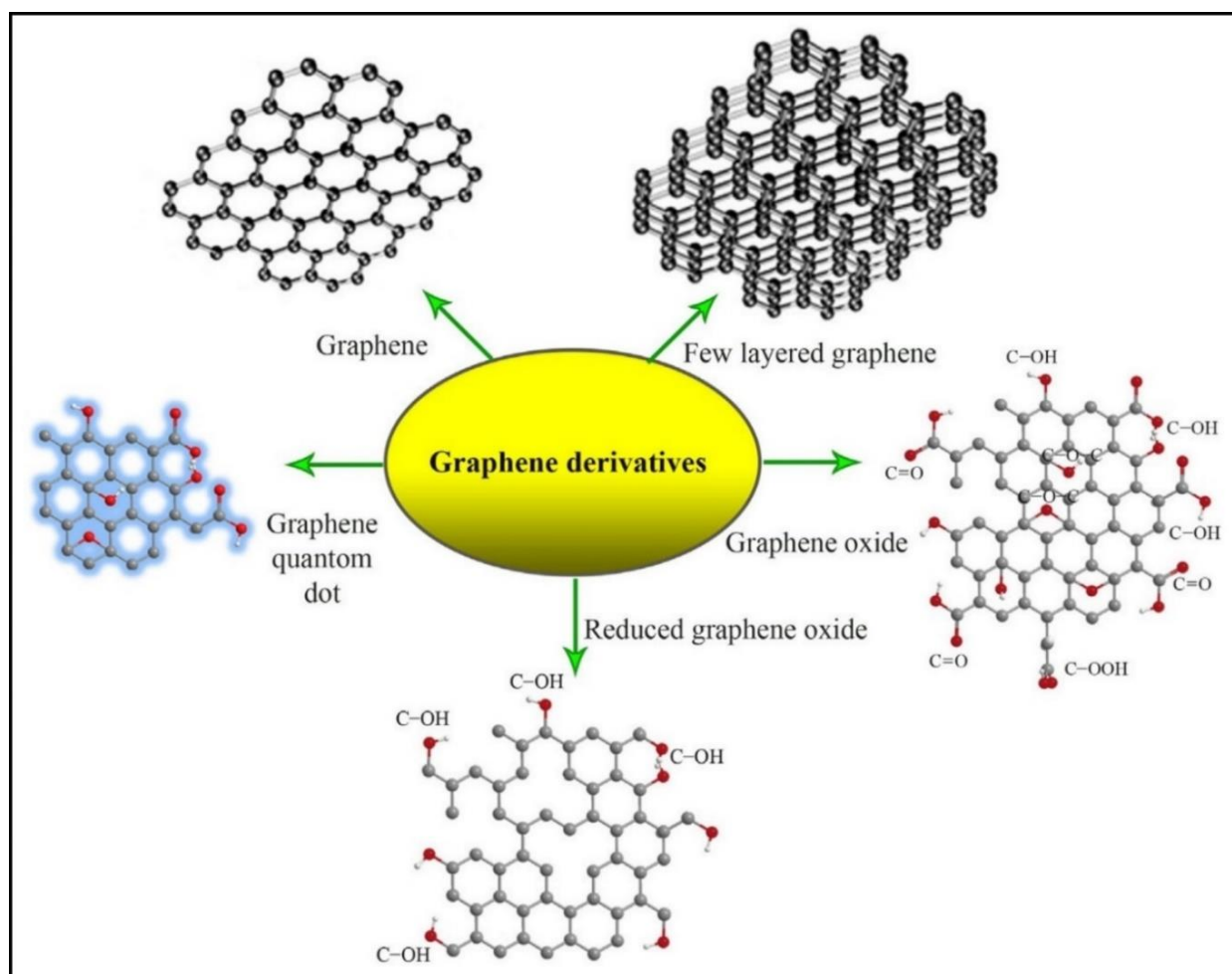


Figure 2. Schematic illustration of various structures of graphene derivatives. Reprinted with permission from Ref. [21].

Because of its extraordinary qualities, graphene is considered to be a better material when compared to other comparable types of materials [22]. Therefore, the consumption of graphene materials has expanded significantly throughout the past several years to meet the specific needs of industry and academia for research and high-performance commercial applications. Graphene derivatives such as graphene oxide (GO) and reduced graphene oxide (rGO) are prominent domains in graphene technological innovation, particularly in terms of commercial applications [23]. The primary goal of this study is to articulate the synthesis methodologies and some significant uses of responsive graphene derivatives towards corrosion prevention, sensor, biomedical, and electroconductive material for energy storage devices.

2. Preparation of Graphene and Its Derivatives

Tour's group at Rice University offered a modification to the Hummers approach; two significant procedures are adopted in the production of graphene [24,25]. It may be classified into two categories: (1) top-down (destruction) and (2) bottom-up (construction) techniques [26]. Graphene synthesis has advanced significantly in recent decades and is now considered an established technique. Regardless of opposition, the "bottom-up" approach involves depositing precursors of carbon onto another substrate as a seed to grow into graphene. This approach also featured as a building technique, and is used to synthesize graphene and its derivatives by utilizing carbon analogs of atomic size besides the graphite to begin the process of graphene formation. Chemical vapor depo-

sition [27,28], gas-phase synthesis without substrate [29] epitaxial growth method [30], template route [31], total organic synthesis [32] and thermal pyrolysis are included in this strategy. Bottom-up procedures are preferred because they can generate almost flawless graphene materials with a high specific surface area, but they are costly and require innovative operating procedures.

The top-down approach involves separating the carbon layer from the massive graphite oxide structure by mechanical/chemical routes or unfolding the graphite structure into a single sheet of graphene [33]. The top-down method, also recognized as a destructive method, involves exfoliating graphite or graphite derivatives to synthesize graphene nanosheets. Oxidative exfoliation-reduction [34], liquid-phase exfoliation [35], mechanical exfoliation [36], arc discharge [37], and carbon nanotube unbuckling [38] are all examples of top-down strategies for separating or unfolding graphite layers into mono and multilayer graphene. In most cases, the top-down approaches are incredibly functional, and the fine-quality of graphene can be synthesized employing these approaches. However, the graphene synthesized by these processes is dependent mainly on the precursor for graphite. They have several drawbacks, such as inconsistent characteristics and limited yields of graphene. Typically, the quality and amount of graphene production are determined by adopting the synthesis process used. According to these two broad categories (top-down and bottom-up), numerous graphene manufacturing processes are already available, as depicted in Figure 3 [39].

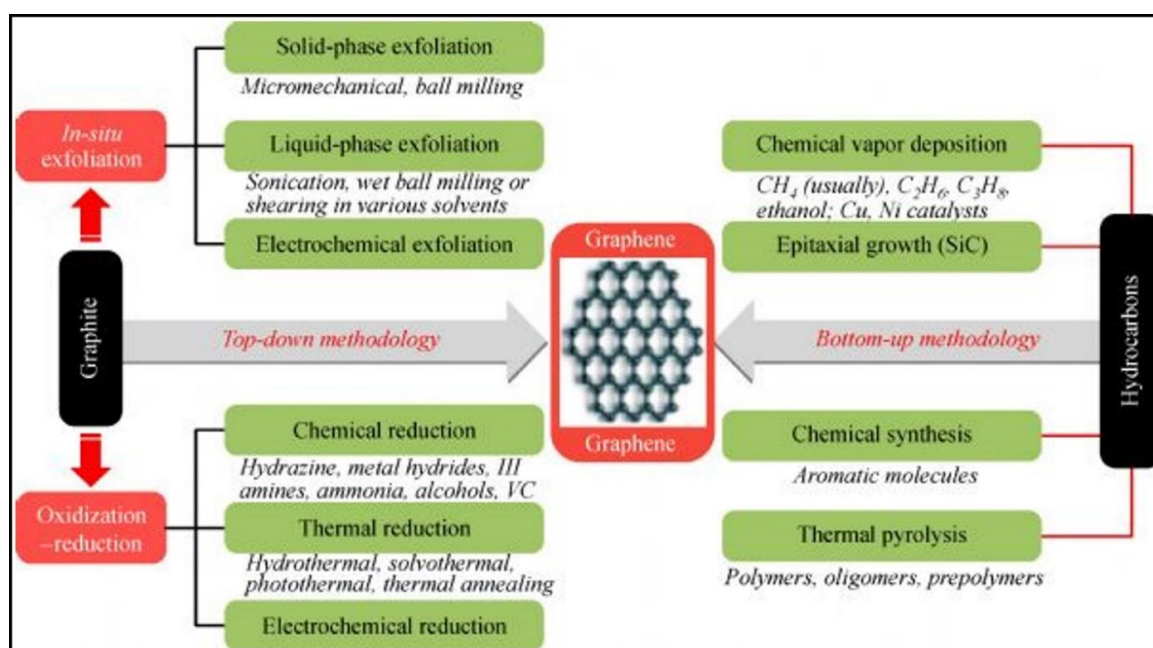


Figure 3. Pathways for graphene production processes (in-situ exfoliation and oxidation reduction) and its utilization by top-down (graphite to graphene) and bottom-up techniques (hydrocarbons to graphene). Reprinted with permission from Ref. [40].

It is possible to synthesize graphene oxide in either a dry or wet environment. In the dry method, graphene is oxidized under an ultrahigh vacuum environment using atomic oxygen, followed by introducing excess molecular oxygen and treatment with ozone under UV radiation. On the other hand, an acceptable strategy is based on the wet synthesis process, under which graphite is commonly employed as a graphene feedstock owing to its natural availability and cost-effectiveness. The three most common reaction pathways are as follows [41]. The first technique involves using graphene that has been generated via a mechanical process and afterward further oxidized. In contrast, the second approach is dependent on exfoliation in aqueous environments utilizing ultrasonic processing [42]. A contemporaneous exfoliation and oxidation approach in a highly acidic media is used

in the Brodie–Staudenmaier–Hummers procedure, which is the third way to take into consideration. As a whole, all of these processes lead to the production of graphene oxide, but the structural properties, such as structure and activation centers of every type of GO, are distinctive.

Brodie [43], Staudenmaier [44], and Hummers in 1958 [45] were three prominent approaches that have been presented in the past centuries. The Tour approach in 2010, for example, was evolved from these basic approaches to increase the total production and quality of the final product. Tour’s group at Rice University proposed a modification to the Hummers approach [7,46]. It was discovered that they could replace sodium nitrite with phosphoric acid in a unique blend of H₂SO₄/H₃PO₄ (9:1) by raising the quantity of KMnO₄ in the mixture. The strength of this strategy is that it does not result in the production of poisonous gases such as NO₂, N₂O₄, or ClO₂ during the whole reaction process, and it is simple to regulate the temperature conditions. According to scientists, the existence of phosphoric acid results in a more consistent graphitic basal plane. An evaluation of the improved synthesis process compared to the old and more sophisticated Hummers’ method is shown in Figure 4. The benefit of the Tour approach is that it produces graphene oxide with a greater hydrophilic extent than the GO obtained by the Hummers method, which is a disadvantage of the Hummers method (Table 1) [41]. Consequently, this graphene oxide becomes more oxidized and dispersible than before. This might be the cause of the various additives that are present. According to tour’s method, reacting in the presence of phosphoric acid can considerably increase the hydrophilic affinity of graphene oxide nanosheets. Table 1 describes the significant synthetic processes associated with the manufacture of GO in comparison with Brodie, Staudenmaier, Sun, Peng and four-step methods [47–51]. Fang et al. [52] reported the formation of mesoporous carbon nanosheets and their derived graphene nanosheets. Figure 5 shows the schematic process for nanosheet formation. In this process, micelles of phenolic resol and Pluronic F-127 were prepared and were then treated with aluminum oxide by a hydrothermal process which was carbonized at 400–500 °C for 2 h. A further thermal treatment at 700 °C for a duration of 2 h and removal of aluminum oxide produced the graphene nanosheets.

In current years, a “primitive” strategy has been developed by a community of scholars, which comprises graphite exfoliation and oxidation in free water with the use of a highly effective oxidizing agent in a protic medium (such as H₂SO₄) [53]. Furthermore, to understand how to effectively optimize these graphene derivatives, graphene and its derivatives have been synthesized via various techniques, which have taken considerable time and effort. Amira Alazmi et al. presented a comparative study on the preparations and reduction routes for GO. In this study, the influence of several graphene oxidation-reduction processes on the morphology and reactivity of rGOs are investigated in depth. To create GO, researchers used two of the most popular oxidation processes described in the literature. Following that, two sets of rGO powders were prepared using three distinct reduction techniques. rGOs are shown to have an extended structural rearrangement that relies not only on the reduction process but also on the method utilized to oxidize the graphite prior to the subsequent oxidation phase [54].

Table 1. Overview of the significant synthetic processes associated with the manufacture of GO [41].

Method	Oxidant	Solvent	Additive	C/O	Resistivity 10 ⁵ Ω·m	Ref.
Brodie	KClO ₃	HNO ₃	-	2.4–2.9	0.15–60	[43,55–59]
Staudenmaier	KClO ₃	Fuming HNO ₃	-	2.2	120	[44,47,57,60]
Hummers	KMnO ₄	H ₂ SO ₄	NaNO ₃	1.8–2.5	0.005–0.01	[45,55,57,61,62]
Tour	KMnO ₄	H ₂ SO ₄	H ₃ PO ₄	0.7–1.3	0.2–1000	[63–65]
Sun	KMnO ₄	H ₂ SO ₄	-	2.5	0.18	[49]
Peng	K ₂ FeMO ₄	H ₂ SO ₄	-	2.2	2.7	[50]
Four-Steps	KMnO ₄	H ₂ SO ₄	-	3.5	23	[51]

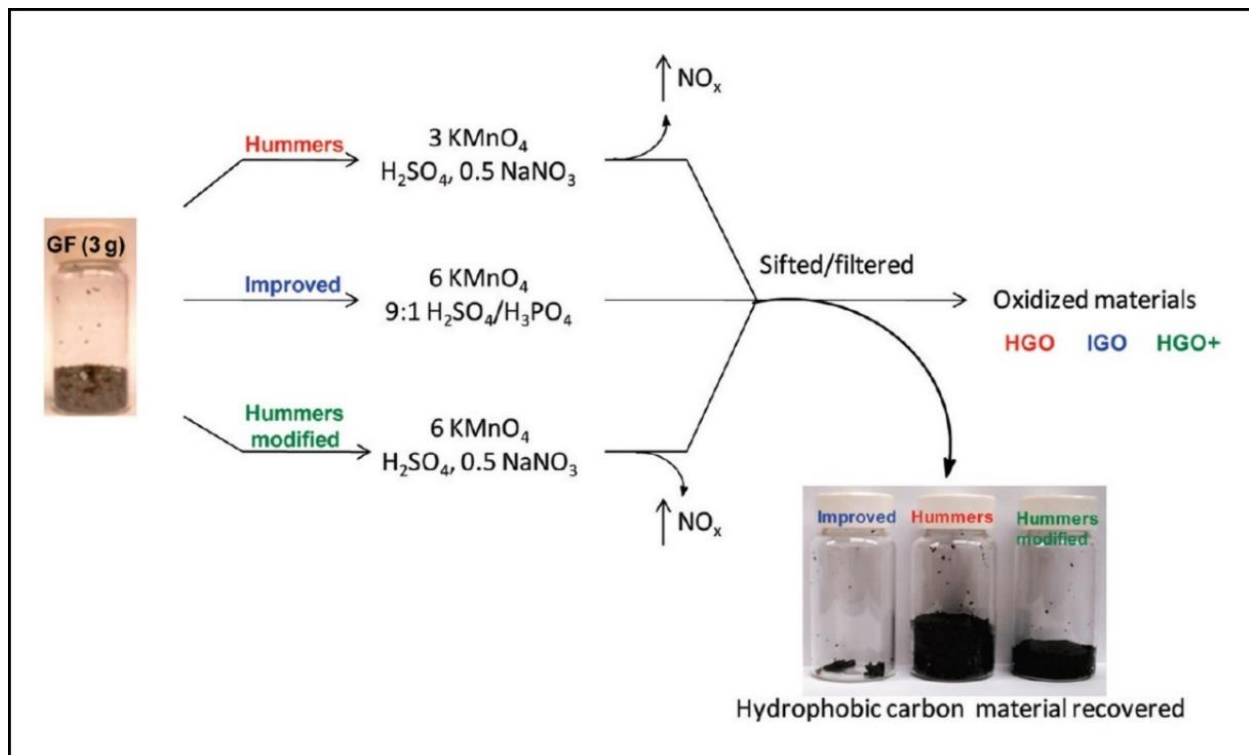


Figure 4. Flowsheet diagram for Tour's method to produce graphene oxide. In this method, graphite serves as the starting material, which is then compared to Hummers and its modification. Displays a carbon source for GO synthesis from graphite. Reprinted with permission from Ref. [63].

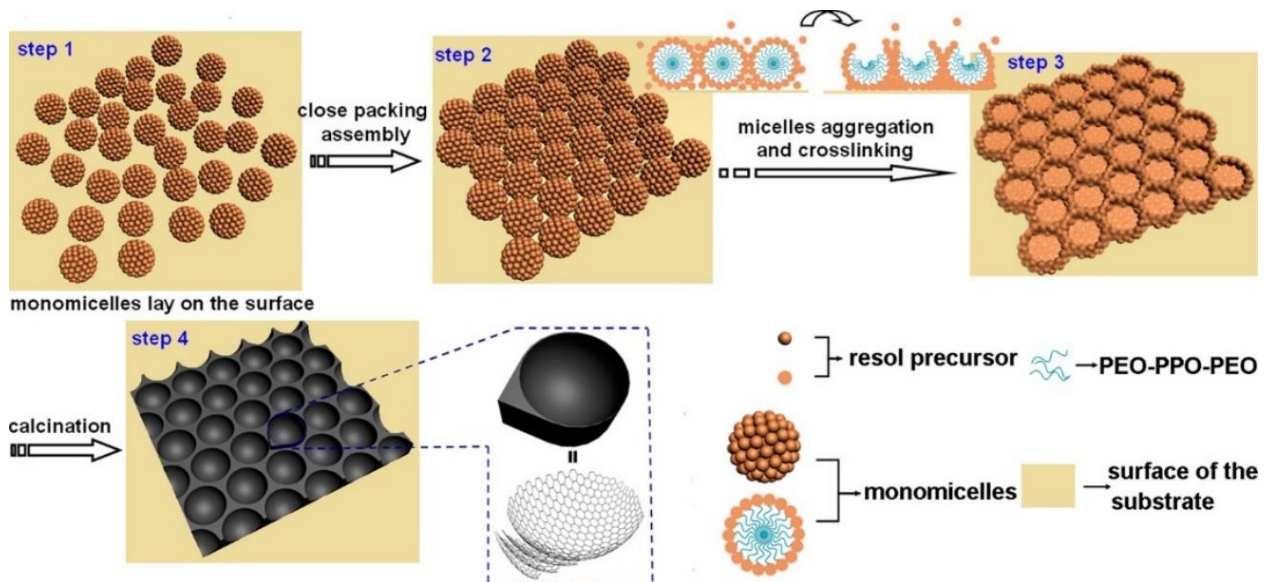


Figure 5. Schematic diagram for the formation of graphene nanosheets. Reprinted with permission from Ref. [52].

3. Potential Energy Storage and Conversion Technologies for a Greener Future

Significant efforts have been undertaken to develop sustainable and clean energy sources and carriers because of global concerns about environmental issues and depletion of natural resources [66–72]. As illustrated in Figure 6, due to its excellent qualities and unique capabilities [73], GO, and its derivatives and composites are being investigated in a number of electrochemical energy storage applications, notably batteries, capacitors, and

fuel cells [73,74]. Examples include GO's ability to operate as an oxidant by reducing its oxygen functional groups and creating composites with GO's unique physical features. In addition, metal or metal oxide nanoparticles may also be anchored to the surface of these structures, negatively charged groups on GO can capture positively charged species for speedier ion transport, as current collector protectors, they may repulse ions with a similar charge to avoid corrosion, and as membrane materials, inhibiting polysulfides diffusion. Moreover, the electro-activity among those functional groups, defects, and edges is relatively high, which can contribute to the acceleration of the kinetics of electrochemical reactions between these two points, the large surface area and the controllable interfacial spacing of thin-layered structures of GO enable electrochemical processes to proceed while simultaneously restricting or mitigating changes in the product's volume [75–77]. An additional feature is that the unoxidized polyaromatic rings can operate as an enabling hydrophobic association (pi-pi layering) and ensure mechanical strength in the presence of carbonaceous sources. The GO surface also has free electrons that can be used as conducting substrates or insulating dielectric spacers depending on the density of oxygen-containing functional groups. The higher density of oxygen-containing groups induces an insulating behavior, while a higher density of electrons makes the material more similar to graphene, ensuring good electrical conduction. The powerful and flexible functions derived from its distinctive shape have emerged as a promising tool in energy systems. It has been used in electrodes, electrocatalysts, safety layers, printing ink, fillers, and membranes, among other applications [78].

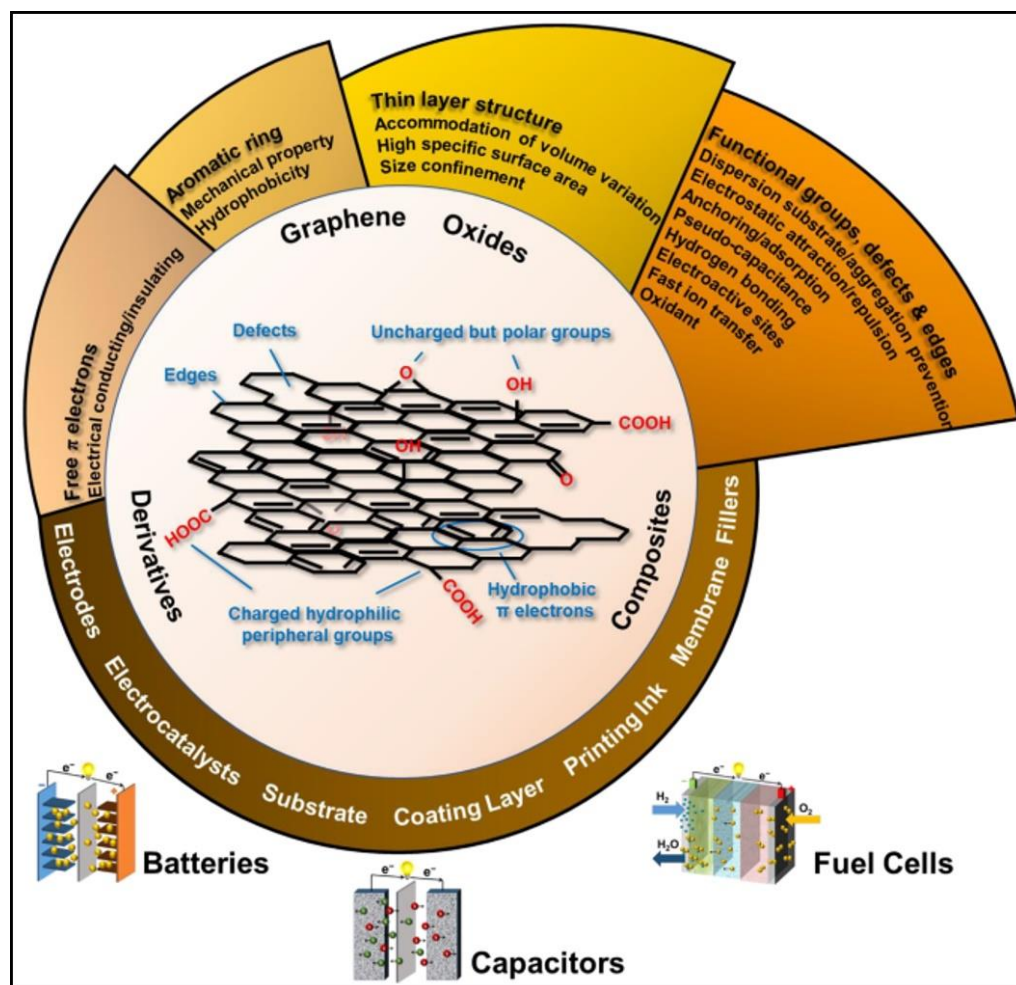


Figure 6. Graphical representation of GO based electrochemical energy storage applications. Reprinted with permission from Ref. [73].

The exceptionally high surface area of GO and rGO allows them to be excellent materials for electrodes to be used for batteries, fuel cells, double-layered capacitors, and solar cells [22,75,79,80]. Compared to certain other graphene materials, the fabrication of GO is more readily upscaled. As a result, it may be employed for energy-related applications in the near future. Lithium-ion batteries that contain nanocomposites of graphene and reduced graphene oxides can accommodate large amounts of energy due to their high capacity. In this particular instance, rGO was coated with metal oxide nanoparticles to enhance the performance of these materials when utilized in battery packs. A Li-ion battery system with an anode material made of reduced graphene oxide covered Fe_3O_4 was constructed. When comparison was made to systems built of pure Fe_3O_4 or Fe_2O_3 , it was observed that the device's energy-storage capacity and exhibited exceptional durability were significantly increased [22,75,76,79–84].

Shahid Rasul and colleagues developed a reasonable model of rGO for the excellent efficiency of supercapacitor electrodes. It was investigated how different oxidation-reduction techniques that are routinely employed might result in significant changes in the efficiency of rGO for supercapacitor applications [85]. Zhu et al. used microwave-assisted exfoliation to produce high-surface-area rGO, therefore lowering the amount of GO required for the manufacture of supercapacitors for utilization in energy storage devices [86]. According to Bo et al. they successfully constructed electronic gas sensors and supercapacitors using the caffeic acid (CA)-rGO and discovered that they had excellent performance for prospective sensors and energy storage applications [87,88].

4. Carbon Dioxide Capture and Storage

Carbon dioxide capture and storage (CCS) is viewed as an effective technique for mitigating the greenhouse effect and the resulting global climate changes [89,90]. To avoid further rises in environmental CO_2 concentrations, CCS innovation [91] has been proposed for all fossil-fuel power stations, which are the principal emitter of Greenhouse gases [92]. Amira Alazmi et al., demonstrated that the surface chemistry and structure of graphite oxide (and, eventually, the reduced version of its components) are mainly reliant on the oxidation environments that the original graphite is confined to during the manufacturing process [92,93]. They explain how GO nanomaterials' have CO_2 adsorption capability, and tunability is affected by their synthesis and drying strategies. As a point of comparison, the GO results are compared to those of two well-known materials: profit-oriented zeolite 13X and a validated reference of single-walled CNTs. The investigation indicated that the modified Hummer's output was outstanding to the other two nanocarbons tested, with a particular surface area of $283 \text{ m}^2/\text{g}$ and a CO_2 uptake capacity of 2.1 mmol/g (at 273 K). The CO_2 adsorption capacity of graphene oxide is influenced by its surface chemistry and roughness [94].

Graphene-based materials (GBM) have excellent properties required for an efficient adsorbent such as functional absorption capacity, pore volume, flexible structure as well as recyclability and energy efficiency [95]. Most of the graphene-based materials used for CO_2 adsorption are reduced graphene oxides which can be easily modified for enhanced thermal, electrical and mechanical properties. These materials show higher CO_2 adsorption ($16.3 \times 10^{-3} \text{ mol/g}$) efficiency because of their heavily interconnected porous structures [95]. Table 2 shows a list of graphene-based materials (GBM) used in carbon capture technology for CO_2 adsorption.

Table 2. List of graphene-based materials (GBM) used for carbon capture technologies for CO₂ adsorption.

No.	GBM	Scale	Conditions	Capacity	Reference
1	Activated graphene derived porous carbon	Large-scale	T = 25 °C; P = 2 MPa	21 × 10 ⁻³ mol/g	[96]
2	Graphene oxide derived carbon	Large-scale	T = 25 °C; P = 2 MPa	16.3 × 10 ⁻³ mol/g	[97]
3	Thermally treated graphene	Large-scale	T = 0 °C; P = 0.1 MPa	2.9 × 10 ⁻³ mol/g	[98]
4	Thermally reduced graphene oxide activated by CO ₂	Large-scale	T = 0 °C; P = 0.1 MPa	3.4 × 10 ⁻³ mol/g	[99]
5	Graphene; Populus wood biomass with KOH activation	Large-scale	T = 0–60 °C; P = 0.1–1 MPa	12.7 × 10 ⁻³ mol/g	[100]
6	Solar reduced graphene oxide	Lab-scale	T = 35 °C; P = 0.1 MPa	1.9 × 10 ⁻³ mol/g	[101]
7	Non-compact graphene	Lab-scale	T = 25 °C; P = 0.14 MPa	117 × 10 ⁻³ mol/g	[102]
8	Steam activated; graphene aerogel	Large-scale	T = 00 °C; P = 0.1 MPa	2.5 × 10 ⁻³ mol/g	[103]
9	Multiply oxidized graphene oxide	-	T = 30 °C; P = 0–1 MPa	3.5 × 10 ⁻³ mol/g	[104]
10	UV irradiated graphene oxide foam	Large-scale	T = 0 °C; P = 0.1 MPa	1.8 × 10 ⁻³ mol/g	[105]

5. Importance in Environmental Pollution and Wastewater Treatment

Air pollution, produced by the industrial production of hazardous gases such as CO, NH₃, NO₂, and CO₂, is one of the most severe dangers to the ecosystem [106,107]. GO can interact with diverse molecules covalently or noncovalently, hence, it can be used in catalysis to transform polluting gases in various industrial processes. Such toxic gases can be eliminated by catching and storing them, catalyzing gas conversion processes, or using them directly [66]. In addition to gas pollution, water pollution is a primary environmental concern. In this field, the use of GO may be separated into two pathways: pollutant adsorption and conversion. Heavy metal ions and organic dyes are the most common water contaminants, and they pose serious harm to humans, aquatic life, animals, and plants [66].

Freshwater scarcity has posed a danger to human life and society's long-term growth, and pollution of current water sources might exacerbate the problem [108,109]. Solar-driven water evaporation is critical for clean water generation by solar purification, and it has lately received more recognition as heat localization technologies have been developed [110–113]. Solar driven water evaporation process is used to get clean water. In this process, the evaporated water is condensed to get pure clean water. However, solar-driven water evaporation may exacerbate the contamination if contaminated water is utilized as the water supply. Figure 7 shows the application of Ag₃PO₄-rGO coated textile for clean water production from solar driven evaporation, decontamination, and disinfection [114]. Application of reduced graphene derived materials' coated textiles not only speed up water evaporation but also act as a catalyst to decontaminate water from various dissolved pollutants and also promotes the disinfection process [114]. Researchers Laila Naureen and colleagues describe the simple fabrication of versatile Ag₃PO₄-rGO nanocomposite coated textiles for freshwater generation through solar-driven evaporation, sterilization, and photocatalysis in this study. The multifunctional materials are made by depositing Ag₃PO₄-rGO nanocomposites onto cotton textile substrates and drying them. It is possible to persist in the water environment, absorb solar radiation, and transform it into heat, increasing the temperature of the surface of the water and boosting water evaporation. The findings revealed that placing Ag₃PO₄-rGO nanocomposite-coated textiles on the water surface and exposing them to solar light irradiation, may accomplish a high water evaporation rate of 1.31 kg/m²h. Moreover, the textiles have the ability to degrade organic dyes and water is also disinfected by the removal of harmful bacteria, resulting in the purification

of wastewater during solar-driven water evaporation. For freshwater production, such a versatile, all-in-one textile provides a long-term but straightforward solution [114].

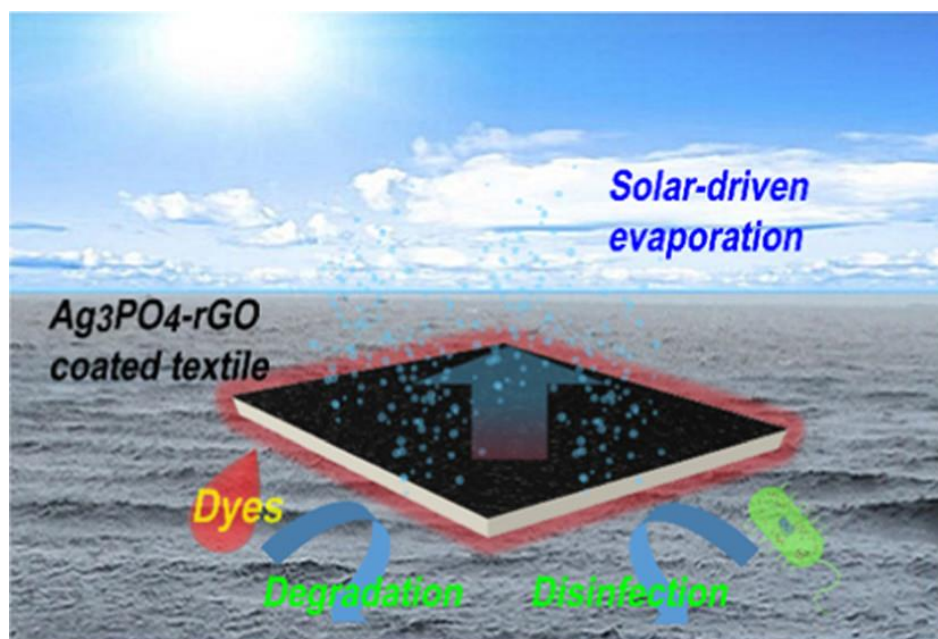


Figure 7. Application of reduced graphene oxide derived Ag_3PO_4 -rGO coated textile in production of clean water by the process of solar evaporation, decontamination and disinfection. Reprinted with permission from Ref. [114].

GO exhibits high adsorption ability towards antimony (III) and (V), cadmium (II), cobalt (II), gold (III), palladium (II), gallium (III), and platinum (IV) [115,116]. Srijita Nundy et al. were successful in fabricating sheet-like, 3D porous material rGO aerogels in order to investigate antimony (Sb) elimination capacity from wastewater [117]. Figure 8 illustrates the whole process for removing Sb (III) and (V) from effluent. The Langmuir isothermal and pseudo-second-order kinetic models best described the adsorption kinetics. At pH 6.0, the highest adsorption capacities of Sb (III) and (V) were 168.59 and 206.72 mg/g, respectively. The thermodynamic characteristics indicated that the reaction was thermodynamically spontaneous, endothermic, and the outcome of dissociative chemisorption. The rGO aerogel provided high selectivity between competing ions and recyclability with a 95% efficacy. When Fixed-bed column studies were conducted utilizing tap water incorporating Sb (III) and (V), rGO demonstrated exemplary practical implementation, removing 97.6% of Sb (III) (3.6 $\mu\text{g}/\text{L}$) and 96.8% of Sb (V) (4.7 $\mu\text{g}/\text{L}$) from both tap water and fixed-bed column experimentation, breakthrough volumes (BV) for the Sb (III) and Sb (V) ions were reported to be 540 BV and 925 BV respectively, until 5 ppb, these are below the requirement of MCL for Sb in drinking water (6 $\mu\text{g}/\text{L}$). The adsorption process was described by XPS and DFT investigations, which showed that Sb (V) had a greater affinity for the rGO surface than Sb (I) (III) [115]. The researchers Klmová et al. investigated the adsorption capacities of GO towards the entire periodic table and found it to be somewhat effective. The ability to adsorb is mainly determined by the process of synthesis. When heated to 293 Kelvin, few-layered graphene oxide nanosheets exhibit an extremely high affinity for Pb (II) ions, with an adsorption capacity of around 842 mg/g. GO has a limited adsorption capability towards Cu (II) ions, even when the oxygen groups on GO serve as binding sites. In addition, graphene oxide has the capability to adsorb additional hazardous water contaminants, such as organic dyes and pesticides [117–119].

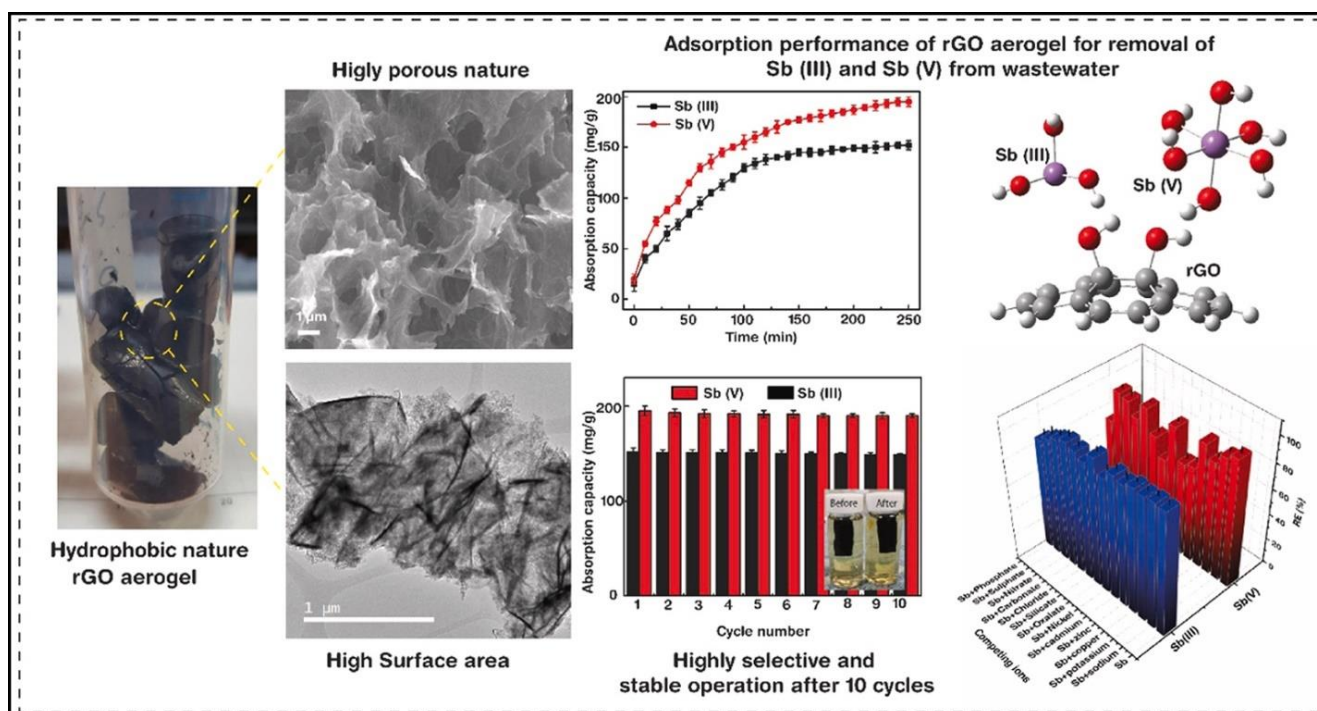


Figure 8. Hydrophobic reduced graphene oxide (rGO) aerogel as highly porous material with high surface area for the removal of antimony from wastewater. Reprinted with permission from Ref. [115].

6. Impact on CO₂ Conversion

CO₂ reduction has become a global scientific challenge because of the rising usage of fossil fuels and their influence on the climate. Value-added feedstock for alternative energy production can be produced using this procedure [120,121]. Using optical energy in conjunction with an external electrical bias, photoelectrocatalysis has the potential to reduce CO₂ emissions significantly. It has attracted particular interest in recent times for its possibility to adjust photoelectrochemical CO₂ reduction. This is due to the fact that graphene is favorable for increasing CO₂ adsorption while also enabling effective electron transfer, and thus monitoring the effectiveness of graphene-based composites. Cheng et al. performed experiments using Pt-amended rGO (Pt-rGO) as the cathode electrocatalyst and Pt-amended TiO₂ nanotubes (Pt-TNTs) as the anode photocatalyst to develop a new photoelectrochemical cell for transforming CO₂ into C₂H₅OH, CH₃COOH, and other products [122]. The Pt-rGO composite material is produced using GO and H₂PtCl₆H₂O salt via a hydrothermal method. The composite is then incorporated into nickel foam after being treated with the catalyst formed during the process. The Pt nanoparticles with a consistent size are uniformly scattered on the surface of rGO and uniformly disseminated on the wall of TNT, indicating that they are both homogeneously dispersed. A photoelectrochemical reactor's efficiency in the absence of CO₂ is investigated in this study, and H₂ is discovered as a sole material, demonstrating that graphene cannot make carbon-containing compounds that combine with really reduced items from CO₂. This catalyst achieves the most effective carbon atom transformation rate of 1130 nmol/h/cm² when used in conjunction with Pt-rGO catalyst, which is sixfold and thrice more remarkable than the rates achieved when using the Pt-CNT and Pt-C catalysts, respectively. When using the Pt-rGO catalyst, a coupled acid and alcohol production rate of 600 nmol/h/cm² is produced, which is much greater than the rates obtained while using the Pt-CNT and Pt-C catalysts 82 nmol/h/cm² and 220 nmol/h/cm², respectively as shown in Figure 9. The exceptional catalytic actions of Pt-rGO can be explained by the fact that rGO exhibits strong reactant absorptivity and excellent charge transfer. According to the results of this study, the specificity of single-carbon products (e.g., CH₃OH, HCOOH) for CO₂ reduction by Pt-rGO remains insufficient. It requires innovation in the study of the emergence, as seen in Figure 9 [122–124].

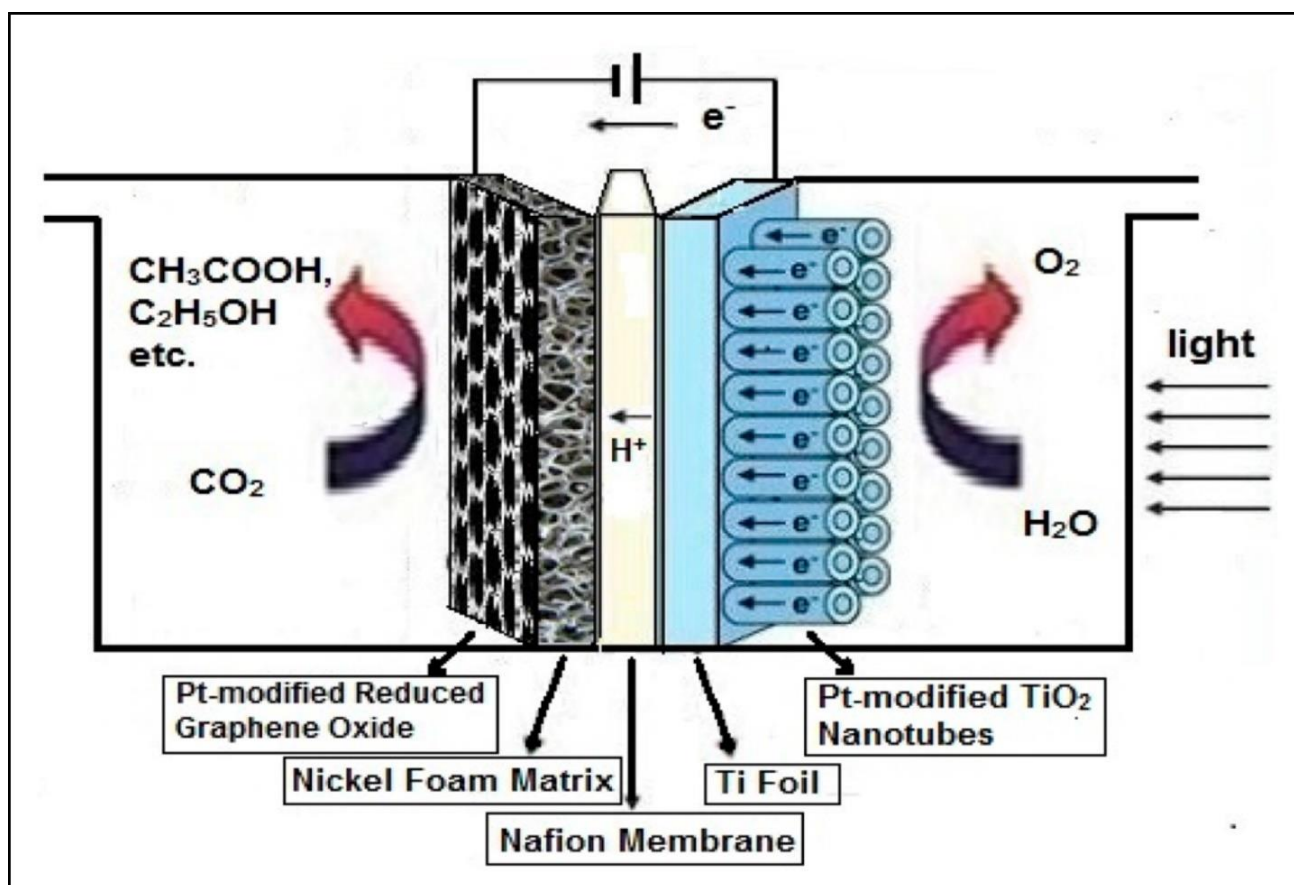


Figure 9. Development of a new photoelectrochemical device for transforming CO₂ into valuable products. Reprinted with permission from Ref. [122].

7. Role in Magnetic Resonance Imaging Contrast Agent

GO has never been explored as a contrast agent for Magnetic Resonance Imaging (MRI) until it was initially envisioned as a diamagnetic material (materials freely magnetizable in a magnetic field) [125]. The similarity in proton density and relaxation times between pathogenic and non-pathologic tissues minimizes signal variability during MRI. A consequence of this is that the MRI contrast is insufficient to allow precise diagnosis [126,127]. Magnetic materials known as MRI contrast agents (MRICA), on the other hand, are able to compensate for this weakness. Because these chemicals alter the magnetic characteristics of specific tissues, the difference between the targeted tissue and the neighboring tissues is enhanced, resulting in improved imaging contrast [126–128]. However, it is possible that introducing structural defects in GO can alter its magnetic response, opening the door for GO to serve as a contrast agent in MRI [129]. GO and its derivatives have been utilized as contrast agents for numerous imaging approaches because of their cellular uptake, superb biocompatibility, bio-conjugation potentials, and feature of absorption throughout a broad wavelength range [126,127,130]. The magnetic characteristics of atomic nuclei form the basis of MRI. In this process, a strong external magnetic field is applied to uniformly align the protons present in the water nuclei of the tissues using an external Radio Frequency (RF) energy. As a result of numerous relaxation processes, the nuclei come to their resting alignment and emit RF energy.

Two different relaxation times for tissues can be described in terms of T₁ and T₂. T₁ stands for longitudinal relaxation time which describes how efficiently excited protons come back to equilibrium. Whereas T₂ stands for transverse relaxation time which describes how efficiently excited protons reach equilibrium. The T₁- and T₂-weighted scans are the most frequent MRI sequences [131]. The magnetic characteristics of RGO samples were

examined by Mahnaz Enayati et al., who discovered that the magnetism in rGO is affected by the competition between structural deficiencies and oxygen capacities to magnetic moments [129]. Amira Alazmi et al. have reported that a GO precursor, which is utilized to generate nanocomposite cobalt ferrite (CoFe_2O_4) and reduced GO, has a significant impact on the relaxing time T_2 , dispersion, magnetic behavior of the molded nanoparticles, and average size. This means that it is possible to double the proton relaxation rate without compromising biocompatibility [132]. Zinia Mohanta et al., have also discussed the effect of oxidation degree of graphene oxide on results of MRI. According to NMR spectroscopy investigation, oxidation levels have a significant impact on GO's nuclear relaxation capabilities, which, in combination with intercalated Mn^{2+} ions, results in a wide range of MRI contrast. This is claimed as the first work to show that GO's relaxivity can be tuned by changing its surface chemistry, which has important implications for the future of creating GO-based contrast agents for use in MRI for diagnostics and therapies [133].

8. Biomedical Applications

Graphene utilization in biological applications is yet another exciting field of research. Because of its vast surface area and chemical stability, graphene is well suited for applications such as medication delivery, gene-altering treatment, DNA patterning, and tissue engineering [134,135]. Graphene was initially used in biological tools to improve medication transmission, which was a breakthrough. In 2008, Sun et al. published the first paper demonstrating the potential of GO as a nano-carrier for drug delivery [136]. Others were encouraged by this discovery to investigate the potential use of graphene materials in the biomedical area in greater depth. A significant portion of surface structure is present on GO. Its enhanced oxygen-containing functional groups give remarkable biocompatibility and solubility qualities, making it a good candidate for drug delivery inside the body [137]. In recent years, researchers have looked into the possibility of using GO to deliver cancer medicines and anti-inflammatory pharmaceuticals [138,139]. Furthermore, the delivery mechanism of GO has made significant strides in the field of chemo-photothermal therapy for cancer treatment [138,139]. To produce ultrasensitive sensors to monitor various biological compounds precisely, functionalized graphene was utilized. These molecules include cholesterol, glucose, hemoglobin, and DNA, among others [78]. Because of the enormous surface area of graphene, it is possible to adsorb proteins onto it. Wang et al. discovered a substantial interfacial contact between the graphene surface and DNA [78]. As part of the DNA tethering procedure, they employed a thick and wrinkled sheet of graphene that had been chemically altered. In addition to its atomic thickness and extraordinarily high thermal and electrical conductivities, the characteristics of graphene make it especially suitable for use in biomolecular imaging [140]. Furthermore, because of their excellent mechanical characteristics, graphene materials have the potential to be used in medicine that promotes the body's own regeneration [78]. Graphene has demonstrated biocompatibility with mammalian cells, which is required for its application as a structural framework in tissue engineering [78,139]. One study discovered that a graphene-based sheet might speed up stem cell development. The mechanical strength of graphene is sufficient to sustain the formation of bone cells such as osteoblasts, constructing it an excellent material for the engineering of bone tissue [78,138,139,141,142]. Figure 10 depicts graphene and its derivatives in the transport of drugs and genetic material. Figure 10 presents a schematic diagram for the utilization of graphene and its derivatives in biomedical applications [143].

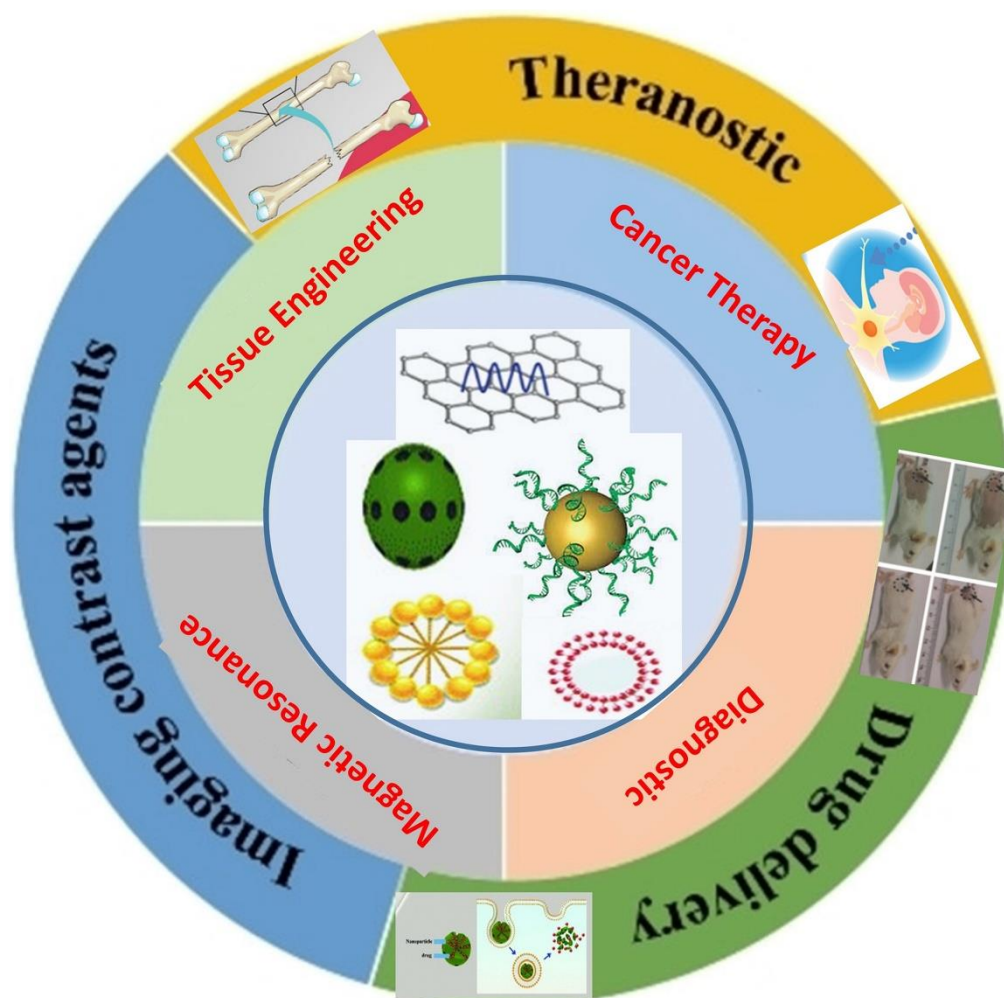


Figure 10. Schematic diagram for the utilization of graphene and its derivatives in the transport of drugs and genetic material. Reprinted with permission from Ref. [143].

In terms of biological applications, GO is extremely helpful in drug delivery systems. Since GO only targets tumors and poses little risks, it is superior to many other cancer treatments since it does not harm healthy cells [141,142]. Successfully prepared nano-GO has been employed in various investigations on the focused medicines for cancer treatment. A camptothecin derivative, SN38, was incorporated onto the polyethylene glycol (PEG)-functionalized nGO (nGO-PEG-SN38) surface. Using this formulation, the medicine is easily dissolved in water and absorbed into the bloodstream [144]. The effectiveness of nGO-PEG-SN38 was much greater than that of irinotecan (CPT-11), a water-soluble SN38 prodrug licensed by the FDA and used to treat colon cancer [144]. In DMSO, the efficacy of nGO-PEG-SN38 was comparable to that of SN38 [144]. Transdermal drug delivery of nGO functionalized with PEG and hyaluronic acid and given photothermal ablation treatment successfully cured mouse melanoma skin cancer. GO was used in some other research to bind magnetite to the anticancer medication doxorubicin hydrochloride, which allowed the medicine to be delivered to precise tumor areas utilizing magnets. Shen et al. investigated the use of GO/rGO in a variety of biomedical applications, with a particular emphasis on drug delivery, cancer treatment, and biological monitoring [142,145,146].

9. Conclusions and Future Outlook

In sophisticated technical applications, the potential and capacities of this material are nearly limitless, thanks to its exceptional physical characteristics. Although the synthesis of graphene and its derivatives has shown to be relatively resilient, the synthesis process

of high-quality graphene on a massive scale remains a complex challenge that must be addressed before the full benefits of this versatile material can be realized in practical uses. According to the research stated before, graphene with a high aspect ratio and a small number of layers is believed to be the most suitable material for use in nanocomposite manufacturing. When designing a futuristic graphene-based polymer look, it is essential to consider the relationship and suitability of graphene derivatives with the polymer matrix. However, there are several obstacles to manufacturing the innovative composite material successfully.

In this review, it was also highlighted how graphene may be employed in a variety of fascinating applications. In recent years, the exceptional physicochemical and mechanical qualities of graphene materials have made them the most suitable materials to replace traditional nanomaterials in polymer matrices. As a result, graphene is now ideal for the production of sensors, biomedical outputs, CCS, wastewater purification, electrical circuits, functional nanomaterials, CO₂ conversion, biomedical applications, magnetic resonance imaging contrast agent, among other applications. Researchers think that in the following decades, graphene will transition from being a purely academic substance to an essential tool for the growth of science and technology, especially in the fields of engineering and manufacturing. It is proposed that future possible implementations will be enhanced, with an emphasis on the following issues.

First, numerous challenging issues of electrochemical energy storage have yet to be resolved despite the extensive research on GO conducted so far. First and foremost, additional research is required to appropriately regulate the microstructures (size and surface chemistry) of GO. The size of GO, including the abundance and transmission of oxygen groups, is highly variable, relying not only on the specific oxidants employed but also the sources of carbon and reactivity parameters. The features of GO are therefore modifiable; nevertheless, how to intentionally tune the properties of GO should be further investigated to enhance the application performance of the technology.

Second, there needs to be more attention paid to understanding how GO interacts with and synergizes with other materials in composites for future energy storage applications. In energy storage devices, the research on GO-based composites is mainly concerned with creating electrodes, solid-state electrolytes, and separators that have exhibited better electrochemical efficiency. Besides elaborating on these findings, in situ nano-characterization methods may help researchers better understand how and why GO-based composites work and how they can be used in conjunction with each other to produce composites that function at their best.

Lastly, the development of new energy storage devices based on graphene and its derivatives should also be pursued in the near future. GO-based materials provide distinct benefits, especially in the fabrication of lithium-ion batteries and supercapacitors. These accomplishments should stimulate greater interest in lithium-sulfur batteries, and metal-ion supercapacitors, among other devices, to investigate the possibility of using GO-derived materials to improve the cycling stability, storage capacity, rate capability of these systems. GO, and its derivatives indeed possess favorable properties in electrochemical applications, and they have a promising and fascinating future ahead of them.

Author Contributions: U.Y.Q. and R.J. made substantial contributions to the conception or design of the work; interpretation of data; the creation of the new software used in the work. He drafted the manuscript and submitted it after thorough revision. All authors have read and agreed to the published version of the manuscript.

Funding: This research received no external funding.

Institutional Review Board Statement: Not applicable.

Informed Consent Statement: Not applicable.

Data Availability Statement: Not applicable.

Conflicts of Interest: The authors declare no conflict of interest.

References

1. University of Manchester Scientists Win the Nobel Prize for Physics. Available online: <https://www.manchester.ac.uk/discover/news/university-of-manchester-scientists-win-the-nobel-prize-for-physics/> (accessed on 6 March 2022).
2. Zhao, S.; Zhao, Z.; Yang, Z.; Ke, L.L.; Kitipornchai, S.; Yang, J. Functionally graded graphene reinforced composite structures: A review. *Eng. Struct.* **2020**, *210*, 110339. [CrossRef]
3. Sun, L.; Xiao, M.; Liu, J.; Gong, K. A study of the polymerization of styrene initiated by K-THF-GIC system. *Eur. Polym. J.* **2006**, *42*, 259–264. [CrossRef]
4. Li, Y.; Zhu, J.; Wei, S.; Ryu, J.; Wang, Q.; Sun, L.; Guo, Z. Poly(propylene) nanocomposites containing various carbon nanostructures. *Macromol. Chem. Phys.* **2011**, *212*, 2429–2438. [CrossRef]
5. Ikram, R.; Jan, B.M.; Ahmad, W. Advances in synthesis of graphene derivatives using industrial wastes precursors; prospects and challenges. *J. Mater. Res. Technol.* **2020**, *9*, 15924–15951. [CrossRef]
6. Papageorgiou, D.G.; Kinloch, I.A.; Young, R.J. Mechanical properties of graphene and graphene-based nanocomposites. *Prog. Mater. Sci.* **2017**, *90*, 75–127. [CrossRef]
7. Dimiev, A.M.; Tour, J.M. Mechanism of graphene oxide formation. *ACS Nano* **2014**, *8*, 3060–3068. [CrossRef]
8. Massetti, M.; Jiao, F.; Ferguson, A.J.; Zhao, D.; Wijeratne, K.; Würger, A.; Blackburn, J.L.; Crispin, X.; Fabiano, S. Unconventional thermoelectric materials for energy harvesting and sensing applications. *Chem. Rev.* **2021**, *121*, 12465–12547. [CrossRef]
9. Kuilla, T.; Bhadra, S.; Yao, D.; Kim, N.H.; Bose, S.; Lee, J.H. Recent advances in graphene based polymer composites. *Prog. Polym. Sci.* **2010**, *35*, 1350–1375. [CrossRef]
10. Smith, A.T.; LaChance, A.M.; Zeng, S.; Liu, B.; Sun, L. Synthesis, properties, and applications of graphene oxide/reduced graphene oxide and their nanocomposites. *Nano Mater. Sci.* **2019**, *1*, 31–47. [CrossRef]
11. Cheng, C.; Li, S.; Thomas, A.; Kotov, N.A.; Haag, R. Functional graphene nanomaterials based architectures: Biointeractions, fabrications, and emerging biological applications. *Chem. Rev.* **2017**, *117*, 1826–1914. [CrossRef]
12. Yoo, B.M.; Shin, H.J.; Yoon, H.W.; Park, H.B. Graphene and graphene oxide and their uses in barrier polymers. *J. Appl. Polym. Sci.* **2014**, *131*, 39628. [CrossRef]
13. Lawal, A.T. Recent progress in graphene based polymer nanocomposites. *Cogent Chem.* **2020**, *6*, 1833476. [CrossRef]
14. Lim, J.V.; Bee, S.T.; Sin, L.T.; Ratnam, C.T.; Hamid, Z.A.A. A Review on the synthesis, properties, and utilities of functionalized carbon nanoparticles for polymer nanocomposites. *Polymers* **2021**, *13*, 3547. [CrossRef]
15. Naskar, A.; Khan, H.; Sarkar, R.; Kumar, S.; Halder, D.; Jana, S. Anti-biofilm activity and food packaging application of room temperature solution process based polyethylene glycol capped Ag-ZnO-graphene nanocomposite. *Mater. Sci. Eng. C* **2018**, *91*, 743–753. [CrossRef]
16. He, Z.; Zhang, S.; Zheng, L.; Liu, Z.; Zhang, G.; Wu, H.; Wang, B.; Liu, Z.; Jin, Z.; Wang, G. Si-based NIR tunneling heterojunction photodetector with interfacial engineering and 3D-Graphene integration. *IEEE Electron Device Lett.* **2022**, *43*, 1818–1821. [CrossRef]
17. Yu, L.; Zhang, S.; Zhang, G.; He, Z.; Feng, X.; Liu, Z.; Wang, G.; Tao, W.; Zheng, L.; Yang, S.; et al. Dual-enhanced photodetectors combining graphene plasmonic nanoresonators with germanium-on-insulator optical cavities. *IEEE Trans. Electron Devices* **2022**, *69*, 3246–3250. [CrossRef]
18. Zhao, Y.; Hao, L.; Zhang, X.; Tan, S.; Li, H.; Zheng, J.; Ji, G. A novel strategy in electromagnetic wave absorbing and shielding materials design: Multi-responsive field effect. *Small Sci.* **2022**, *2*, 2100077. [CrossRef]
19. Liu, Q.; Wang, Z.; Han, E.H.; Wang, S.; Chang, J. Effect of cyanate ester and graphene oxide as modifiers on corrosion protection performance of epoxy composite coating in sulfuric acid solution. *Corros. Sci.* **2021**, *182*, 109266. [CrossRef]
20. Junaidi, N.F.D.; Othman, N.H.; Fuzil, N.S.; Mat Shayuti, M.S.; Alias, N.H.; Shahrudin, M.Z.; Marpani, F.; Lau, W.J.; Ismail, A.F.; Aba, N.F.D. Recent development of graphene oxide-based membranes for oil–water separation: A review. *Sep. Purif. Technol.* **2021**, *258*, 118000. [CrossRef]
21. Ramezani, M.; Alibolandi, M.; Nejabat, M.; Charbgo, F.; Taghdisi, S.M.; Abnous, K. Graphene-based hybrid nanomaterials for biomedical applications. In *Biomedical Applications of Graphene and 2D Nanomaterials*; Elsevier: Amsterdam, The Netherlands, 2019; pp. 119–141. [CrossRef]
22. Obodo, R.M.; Ramzan, M.; Nsude, H.E.; Onoh, E.U.; Ahmad, I.; Maaza, M.; Ezema, F.I. Radiations induced defects in electrode materials for energy storage devices. *Radiat. Phys. Chem.* **2022**, *191*, 109838. [CrossRef]
23. Razaq, A.; Bibi, F.; Zheng, X.; Papadakis, R.; Jafri, S.H.M.; Li, H. Review on graphene-, graphene oxide-, reduced graphene oxide-based flexible composites: From fabrication to applications. *Materials* **2022**, *15*, 1012. [CrossRef] [PubMed]
24. Sinitskii, A.; Tour, J.M. *Chemical approaches to produce graphene oxide and related materials. Graphene Nanoelectronics From Materials to Circuits*; Springer: Boston, MA, USA, 2012; pp. 205–234. [CrossRef]
25. Ikram, R.; Jan, B.M.; Ahmad, W. An overview of industrial scalable production of graphene oxide and analytical approaches for synthesis and characterization. *J. Mater. Res. Technol.* **2020**, *9*, 11587–11610. [CrossRef]
26. Edwards, R.S.; Coleman, K.S. Graphene synthesis: Relationship to applications. *Nanoscale* **2012**, *5*, 38–51. [CrossRef]
27. Son, M.; Ham, M.H. Low-temperature synthesis of graphene by chemical vapor deposition and its applications. *FlatChem* **2017**, *5*, 40–49. [CrossRef]
28. Dato, A.; Frenklach, M. Substrate-free microwave synthesis of graphene: Experimental conditions and hydrocarbon precursors. *New J. Phys.* **2010**, *12*, 125013. [CrossRef]

29. Jacobberger, R.M.; Machhi, R.; Wroblewski, J.; Taylor, B.; Gillian-Daniel, A.L.; Arnold, M.S. Simple graphene synthesis via chemical vapor deposition. *J. Chem. Educ.* **2015**, *92*, 1903–1907. [[CrossRef](#)]
30. Huang, H.; Chen, S.; Wee, A.T.S.; Chen, W. Epitaxial growth of graphene on silicon carbide (SiC). In *Graphene Properties, Preparation, Characterisation and Applications*; Woodhead Publishing: Sawston, UK, 2014; pp. 177–198. [[CrossRef](#)]
31. Yang, Y.; Liu, R.; Wu, J.; Jiang, X.; Cao, P.; Hu, X.; Pan, T.; Qiu, C.; Yang, J.; Song, Y.; et al. Bottom-up fabrication of graphene on silicon/silica substrate via a facile soft-hard template approach. *Sci. Rep.* **2015**, *5*, 13480. [[CrossRef](#)]
32. Singh, V.; Joung, D.; Zhai, L.; Das, S.; Khondaker, S.I.; Seal, S. Graphene based materials: Past, present and future. *Prog. Mater. Sci.* **2011**, *56*, 1178–1271. [[CrossRef](#)]
33. Zhang, R.; Yu, X.; Yang, Q.; Cui, G.; Li, Z. The role of graphene in anti-corrosion coatings: A review. *Constr. Build. Mater.* **2021**, *294*, 123613. [[CrossRef](#)]
34. Shen, L.; Zhang, L.; Wang, K.; Miao, L.; Lan, Q.; Jiang, K.; Lu, H.; Li, M.; Li, Y.; Shen, B.; et al. Analysis of oxidation degree of graphite oxide and chemical structure of corresponding reduced graphite oxide by selecting different-sized original graphite. *RSC Adv.* **2018**, *8*, 17209–17217. [[CrossRef](#)]
35. Haar, S.; Bruna, M.; Lian, J.X.; Tomarchio, F.; Olivier, Y.; Mazzaro, R.; Morandi, V.; Moran, J.; Ferrari, A.C.; Beljonne, D.; et al. Liquid-phase exfoliation of graphite into single- and few-layer graphene with α -functionalized alkanes. *J. Phys. Chem. Lett.* **2016**, *7*, 2714–2721. [[CrossRef](#)] [[PubMed](#)]
36. Novoselov, K.S.; Geim, A.K.; Morozov, S.V.; Jiang, D.; Zhang, Y.; Dubonos, S.V.; Grigorieva, I.V.; Firsov, A.A. Electric field in atomically thin carbon films. *Science* **2004**, *306*, 666–669. [[CrossRef](#)] [[PubMed](#)]
37. Pham, T.V.; Kim, J.G.; Jung, J.Y.; Kim, J.H.; Cho, H.; Seo, T.H.; Lee, H.; Kim, N.D.; Kim, M.J. High areal capacitance of N-doped graphene synthesized by Arc discharge. *Adv. Funct. Mater.* **2019**, *29*, 1905511. [[CrossRef](#)]
38. Zhao, K.; Zhang, T.; Chang, H.; Yang, Y.; Xiao, P.; Zhang, H.; Li, C.; Tiwary, C.S.; Ajayan, P.M.; Chen, Y. Super-elasticity of three-dimensionally cross-linked graphene materials all the way to deep cryogenic temperatures. *Sci. Adv.* **2019**, *5*, eaav2589. [[CrossRef](#)] [[PubMed](#)]
39. Coroş, M.; Pogăcean, F.; Măgeruşan, L.; Socaci, C.; Pruneanu, S. A brief overview on synthesis and applications of graphene and graphene-based nanomaterials. *Front. Mater. Sci.* **2019**, *13*, 23–32. [[CrossRef](#)]
40. Yang, Y.; Han, C.; Jiang, B.; Iocozzia, J.; He, C.; Shi, D.; Jiang, T.; Lin, Z. Graphene-based materials with tailored nanostructures for energy conversion and storage. *Mater. Sci. Eng. R Rep.* **2016**, *102*, 1–72. [[CrossRef](#)]
41. Pendolino, F.; Armata, N. *Graphene Oxide in Environmental Remediation Process*; Springer: Cham, Switzerland, 2017; Volume 7, ISBN 978-3-319-60428-2.
42. Sandhya, M.; Ramasamy, D.; Sudhakar, K.; Kadirgama, K.; Harun, W.S.W. Ultrasonication an intensifying tool for preparation of stable nanofluids and study the time influence on distinct properties of graphene nanofluids—A systematic overview. *Ultrason. Sonochem.* **2021**, *73*, 105479. [[CrossRef](#)]
43. Collins Brodie, B. XIII. On the atomic weight of graphite. *Philos. Trans. R. Soc. Lond.* **1859**, *149*, 249–259. [[CrossRef](#)]
44. Staudenmaier, L. Verfahren zur Darstellung der Graphitsäure. *Ber. Der Dtsch. Chem. Ges.* **1898**, *31*, 1481–1487. [[CrossRef](#)]
45. Hummers, W.S.; Offeman, R.E. Preparation of graphitic oxide. *J. Am. Chem. Soc.* **2002**, *80*, 1339. [[CrossRef](#)]
46. Marcano, D.C.; Kosynkin, D.V.; Berlin, J.M.; Sinitskii, A.; Sun, Z.; Slesarev, A.; Alemany, L.B.; Lu, W.; Tour, J.M. Improved synthesis of graphene oxide. *ACS Nano* **2010**, *4*, 4806–4814. [[CrossRef](#)] [[PubMed](#)]
47. Poh, H.L.; Sanek, F.; Ambrosi, A.; Zhao, G.; Sofer, Z.; Pumera, M. Graphenes prepared by Staudenmaier, Hofmann and Hummers methods with consequent thermal exfoliation exhibit very different electrochemical properties. *Nanoscale* **2012**, *4*, 3515–3522. [[CrossRef](#)] [[PubMed](#)]
48. Zaaba, N.I.; Foo, K.L.; Hashim, U.; Tan, S.J.; Liu, W.; Voon, C.H. Synthesis of Graphene Oxide using Modified Hummers Method: Solvent Influence. *Procedia Engineering* **2017**, *184*, 469–477. [[CrossRef](#)]
49. Sun, L.; Fugetsu, B. Mass production of graphene oxide from expanded graphite. *Mater. Lett.* **2013**, *109*, 207–210. [[CrossRef](#)]
50. Peng, L.; Xu, Z.; Liu, Z.; Wei, Y.; Sun, H.; Li, Z.; Zhao, X.; Gao, C. An iron-based green approach to 1-h production of single-layer graphene oxide. *Nat. Commun.* **2015**, *6*, 5716. [[CrossRef](#)]
51. Pendolino, F.; Armata, N.; Masullo, T.; Cuttitta, A. Temperature influence on the synthesis of pristine graphene oxide and graphite oxide. *Mater. Chem. Phys.* **2015**, *164*, 71–77. [[CrossRef](#)]
52. Fang, Y.; Lv, Y.; Che, R.; Wu, H.; Zhang, X.; Gu, D.; Zheng, G.; Zhao, D. Two-dimensional mesoporous carbon nanosheets and their derived graphene nanosheets: Synthesis and efficient lithium ion storage. *J. Am. Chem. Soc.* **2013**, *135*, 1524–1530. [[CrossRef](#)]
53. Wang, J.; Wang, Y.; Zhang, Y.; Uliana, A.; Zhu, J.; Liu, J.; Van Der Bruggen, B. Zeolitic imidazolate framework/graphene oxide hybrid nanosheets functionalized thin film nanocomposite membrane for enhanced antimicrobial performance. *ACS Appl. Mater. Interfaces* **2016**, *8*, 25508–25519. [[CrossRef](#)]
54. Alazmi, A.; Rasul, S.; Patole, S.P.; Costa, P.M.F.J. Comparative study of synthesis and reduction methods for graphene oxide. *Polyhedron* **2016**, *116*, 153–161. [[CrossRef](#)]
55. You, S.; Luzan, S.M.; Szabó, T.; Talyzin, A.V. Effect of synthesis method on solvation and exfoliation of graphite oxide. *Carbon* **2013**, *52*, 171–180. [[CrossRef](#)]
56. Shin, H.J.; Kim, K.K.; Benayad, A.; Yoon, S.M.; Park, H.K.; Jung, I.S.; Jin, M.H.; Jeong, H.K.; Kim, J.M.; Choi, J.Y.; et al. Efficient reduction of graphite oxide by sodium borohydride and its effect on electrical conductance. *Adv. Funct. Mater.* **2009**, *19*, 1987–1992. [[CrossRef](#)]

57. Scholz, W.; Boehm, H.P. Untersuchungen am Graphitoxid. VI. Betrachtungen zur Struktur des Graphitoxids. *ZAAC-J. Inorg. Gen. Chem.* **1969**, *369*, 327–340. [\[CrossRef\]](#)
58. Schniepp, H.C.; Li, J.L.; McAllister, M.J.; Sai, H.; Herrera-Alonson, M.; Adamson, D.H.; Prud'homme, R.K.; Car, R.; Seville, D.A.; Aksay, I.A. Functionalized single graphene sheets derived from splitting graphite oxide. *J. Phys. Chem. B* **2006**, *110*, 8535–8539. [\[CrossRef\]](#) [\[PubMed\]](#)
59. Feicht, P.; Biskupek, J.; Gorelik, T.E.; Renner, J.; Halbig, C.E.; Maranska, M.; Puchtler, F.; Kaiser, U.; Eigler, S. Brodie's or Hummers' Method: Oxidation Conditions Determine the Structure of Graphene Oxide. *Chem. Eur. J.* **2019**, *25*, 8955–8959. [\[CrossRef\]](#)
60. Ma, H.-L.; Zhang, H.-B.; Hu, Q.-H.; Li, W.-J.; Jiang, Z.-G.; Yu, Z.-Z.; Dasari, A. Functionalization and reduction of graphene oxide with p-phenylene diamine for electrically conductive and thermally stable polystyrene composites. *ACS Appl. Mater. Interfaces* **2012**, *4*, 1948–1953. [\[CrossRef\]](#) [\[PubMed\]](#)
61. Stankovich, S.; Dikin, D.A.; Piner, R.D.; Kohlhaas, K.A.; Kleinhammes, A.; Jia, Y.; Wu, Y.; Nguyen, S.B.T.; Ruoff, R.S. Synthesis of graphene-based nanosheets via chemical reduction of exfoliated graphite oxide. *Carbon* **2007**, *45*, 1558–1565. [\[CrossRef\]](#)
62. Jung, I.; Field, D.A.; Clark, N.J.; Zhu, Y.; Yang, D.; Piner, R.D.; Stankovich, S.; Dikin, D.A.; Geisler, H.; Ventrice, C.A.; et al. Reduction kinetics of graphene oxide determined by electrical transport measurements and temperature programmed desorption. *J. Phys. Chem. C* **2009**, *113*, 18480–18486. [\[CrossRef\]](#)
63. Kotsyubynsky, V.O.; Boychuk, V.M.; Budzulyak, I.M.; Rachiy, B.I.; Hodlevska, M.A.; Kachmar, A.I.; Hodlevsky, M.A. Graphene oxide synthesis using modified Tour method. *Adv. Nat. Sci. Nanosci. Nanotechnol.* **2021**, *12*, 035006. [\[CrossRef\]](#)
64. Gilje, S.; Han, S.; Wang, M.; Wang, K.L.; Kaner, R.B. A chemical route to graphene for device applications. *Nano Lett.* **2007**, *7*, 3394–3398. [\[CrossRef\]](#)
65. Kovtyukhova, N.I.; Ollivier, P.J.; Martin, B.R.; Mallouk, T.E.; Buzaneva, E.V.; Gorchinskiy, A.D. Layer-by-layer assembly of ultrathin composite films from micron-sized graphite oxide sheets and polycations. *Chem. Mater.* **1999**, *11*, 771–778. [\[CrossRef\]](#)
66. Li, F.; Jiang, X.; Zhao, J.; Zhang, S. Graphene oxide: A promising nanomaterial for energy and environmental applications. *Nano Energy* **2015**, *16*, 488–515. [\[CrossRef\]](#)
67. Javaid, R.; Nanba, T. Effect of preparation method and reaction parameters on catalytic activity for ammonia synthesis. *Int. J. Hydrogen Energy* **2021**, *46*, 35209–35218. [\[CrossRef\]](#)
68. Afzal, A.; Ahmad Abuilaiwi, F.; Javaid, R.; Ali, F.; Habib, A. Solid-state synthesis of heterogeneous $\text{Ni}_{0.5}\text{Cu}_{0.5-x}\text{Zn}_x\text{Fe}_2\text{O}_4$ spinel oxides with controlled morphology and tunable dielectric properties. *J. Mater. Sci. Mater. Electron.* **2020**, *31*, 14261–14270. [\[CrossRef\]](#)
69. Yaqub Qazi, U.; Javaid, R.; Tahir, N.; Jamil, A.; Afzal, A. Design of advanced self-supported electrode by surface modification of copper foam with transition metals for efficient hydrogen evolution reaction. *Int. J. Hydrogen Energy* **2020**, *45*, 33396–33406. [\[CrossRef\]](#)
70. Javaid, R.; Nanba, T.; Matsumoto, H. Kinetic analysis of ammonia production on Ru catalyst under high pressure conditions. In *CO₂ Free Ammonia as an Energy Carrier*; Aika, K., Kobayashi, H., Eds.; Springer: Singapore, 2023; pp. 279–286.
71. Kobayashi, K.; Javaid, R.; Manaka, Y.; Nanba, T.; Nishi, M.; Mochizuki, T.; Chen, S.; Takagi, H. Comparison of several ammonia catalysts worked under industrial conditions. In *CO₂ Free Ammonia as an Energy Carrier*; Aika, K., Kobayashi, H., Eds.; Springer: Singapore, 2023; pp. 263–278.
72. Javaid, R.; Nanba, T. Ru/CeO₂/MgO catalysts for enhanced ammonia synthesis efficiency. *Top. Catal.* **2023**. [\[CrossRef\]](#)
73. Tian, Y.; Yu, Z.; Cao, L.; Zhang, X.L.; Sun, C.; Wang, D.W. Graphene oxide: An emerging electromaterial for energy storage and conversion. *J. Energy Chem.* **2021**, *55*, 323–344. [\[CrossRef\]](#)
74. Azam, M.A.; Seman, R.N.A.R. Application of graphene in supercapacitors, batteries, and fuel cells. In *Graphene, Nanotubes and Quantum Dots-Based Nanotechnology*; Woodhead Publishing: Sawston, UK, 2022; pp. 209–231. [\[CrossRef\]](#)
75. Liu, J.-B.; Gong, H.-S.; Ye, G.-L.; Fei, H.-L. Graphene oxide-derived single-atom catalysts for electrochemical energy conversion. *Rare Met.* **2022**, *41*, 1703–1726. [\[CrossRef\]](#)
76. Li, J.; Ding, Z.; Li, J.; Wang, C.; Pan, L.; Wang, G. Synergistic coupling of NiS_{1.03} nanoparticle with S-doped reduced graphene oxide for enhanced lithium and sodium storage. *Chem. Eng. J.* **2021**, *407*, 127199. [\[CrossRef\]](#)
77. Qazi, U.Y.; Javaid, R.; Zahid, M.; Tahir, N.; Afzal, A.; Lin, X.M. Bimetallic NiCo–NiCoO₂ nano-heterostructures embedded on copper foam as a self-supported bifunctional electrode for water oxidation and hydrogen production in alkaline media. *Int. J. Hydrogen Energy* **2021**, *46*, 18936–18948. [\[CrossRef\]](#)
78. Wang, Y.; Li, Z.; Wang, J.; Li, J.; Lin, Y. Graphene and graphene oxide: Biofunctionalization and applications in biotechnology. *Trends Biotechnol.* **2011**, *29*, 205–212. [\[CrossRef\]](#)
79. Kumar, R.; Thangappan, R. Electrode material based on reduced graphene oxide (rGO)/transition metal oxide composites for supercapacitor applications: A review. *Emergent Mater.* **2022**, *5*, 1881–1897. [\[CrossRef\]](#)
80. Wang, S.; Cao, K.; Xu, L.; Zhao, D.; Tong, Y. Carbon nanotubes/reduced graphene oxide composites as electrode materials for supercapacitors. *Appl. Phys. A Mater. Sci. Process.* **2022**, *128*, 81. [\[CrossRef\]](#)
81. Folorunso, O.; Sadiku, R.; Hamam, Y.; Ray, S.S. An investigation of copper oxide-loaded reduced graphene oxide nanocomposite for energy storage applications. *Appl. Phys. A Mater. Sci. Process.* **2022**, *128*, 54. [\[CrossRef\]](#)
82. Ramesh, S.; Karuppasamy, K.; Vikraman, D.; Santhoshkumar, P.; Bathula, C.; Palem, R.R.; Kathalingam, A.; Kim, H.S.; Kim, J.H.; Kim, H.S. Sheet-like morphology CuCo₂O₄ bimetallic nanoparticles adorned on graphene oxide composites for symmetrical energy storage applications. *J. Alloys Compd.* **2022**, *892*, 162182. [\[CrossRef\]](#)

83. Zhao, C.; Shao, X.; Zhang, Y.; Qian, X. Fe₂O₃/Reduced graphene Oxide/Fe₃O₄ composite in situ grown on Fe foil for high-performance supercapacitors. *ACS Appl. Mater. Interfaces* **2016**, *8*, 30133–30142. [[CrossRef](#)]
84. SAzmi, S.; Koudahi, M.F.; Frackowiak, E. Reline deep eutectic solvent as a green electrolyte for electrochemical energy storage applications. *Energy Environ. Sci.* **2022**, *15*, 1156–1171. [[CrossRef](#)]
85. Rasul, S.; Alazmi, A.; Jaouen, K.; Hedhili, M.N.; Costa, P.M.F.J. Rational design of reduced graphene oxide for superior performance of supercapacitor electrodes. *Carbon* **2017**, *111*, 774–781. [[CrossRef](#)]
86. Zhu, Y.; Murali, S.; Stoller, M.D.; Velamakanni, A.; Piner, R.D.; Ruoff, R.S. Microwave assisted exfoliation and reduction of graphite oxide for ultracapacitors. *Carbon* **2010**, *48*, 2118–2122. [[CrossRef](#)]
87. Bo, Z.; Shuai, X.; Mao, S.; Yang, H.; Qian, J.; Chen, J.; Yan, J.; Cen, K. Green preparation of reduced graphene oxide for sensing and energy storage applications. *Sci. Rep.* **2014**, *4*, 4684. [[CrossRef](#)]
88. Javaid, R.; Nanba, T. Effect of reaction conditions and surface characteristics of Ru/CeO₂ on catalytic performance for ammonia synthesis as a clean fuel. *Int. J. Hydrogen Energy* **2021**, *46*, 18107–18115. [[CrossRef](#)]
89. Javaid, R.; Matsumoto, H.; Nanba, T. Influence of reaction conditions and promoting role of ammonia produced at higher temperature conditions in its synthesis process over Cs-Ru/MgO catalyst. *ChemistrySelect* **2019**, *4*, 2218–2224. [[CrossRef](#)]
90. Yaqub Qazi, U.; Javaid, R. A review on metal nanostructures: Preparation methods and their potential applications. *Adv. Nanopart.* **2016**, *05*, 27–43. [[CrossRef](#)]
91. Lichtschlag, A.; Pearce, C.R.; Suominen, M.; Blackford, J.; Borisov, S.M.; Bull, J.M.; de Beer, D.; Dean, M.; Esposito, M.; Flohr, A.; et al. Suitability analysis and revised strategies for marine environmental carbon capture and storage (CCS) monitoring. *Int. J. Greenh. Gas Control* **2021**, *112*, 103510. [[CrossRef](#)]
92. Ahmed, R.; Liu, G.; Yousaf, B.; Abbas, Q.; Ullah, H.; Ali, M.U. Recent advances in carbon-based renewable adsorbent for selective carbon dioxide capture and separation—A review. *J. Clean. Prod.* **2020**, *242*, 118409. [[CrossRef](#)]
93. Raza, A.; Gholami, R.; Rezaee, R.; Rasouli, V.; Rabiei, M. Significant aspects of carbon capture and storage—A review. *Petroleum* **2019**, *5*, 335–340. [[CrossRef](#)]
94. Alazmi, A.; El Tall, O.; Hedhili, M.N.; Costa, P.M.F.J. The impact of surface chemistry and texture on the CO₂ uptake capacity of graphene oxide. *Inorg. Chim. Acta* **2018**, *482*, 470–477. [[CrossRef](#)]
95. Sreedhar, I.; Upadhyay, U.; Roy, P.; Thodur, S.M.; Patel, C.M. Carbon capture and utilization by graphenes-path covered and ahead. *J. Clean. Prod.* **2021**, *284*, 124712. [[CrossRef](#)]
96. Ganesan, A.; Shaijumon, M.M. Activated graphene-derived porous carbon with exceptional gas adsorption properties. *Microporous Mesoporous Mater.* **2016**, *220*, 21–27. [[CrossRef](#)]
97. Srinivas, G.; Burrell, J.; Yildirim, T. Graphene oxide derived carbons (GODCs): Synthesis and gas adsorption properties. *Energy Environ. Sci.* **2012**, *5*, 6453–6459. [[CrossRef](#)]
98. Chowdhury, S.; Balasubramanian, R. Highly efficient, rapid and selective CO₂ capture by thermally treated graphene nanosheets. *J. CO₂ Util.* **2016**, *13*, 50–60. [[CrossRef](#)]
99. Chowdhury, S.; Balasubramanian, R. Three-dimensional graphene-based porous adsorbents for postcombustion CO₂ capture. *Ind. Eng. Chem. Res.* **2016**, *55*, 7906–7916. [[CrossRef](#)]
100. Ekhlesi, L.; Younesi, H.; Rashidi, A.; Bahramifar, N. Populus wood biomass-derived graphene for high CO₂ capture at atmospheric pressure and estimated cost of production. *Process Saf. Environ. Prot.* **2018**, *113*, 97–108. [[CrossRef](#)]
101. Nagarajan, L.; Sampath Kumar, P.; Arulraj, A.; Senguttuvan, G.; Kumaraguru, K. Solar assisted reduced graphene oxide as adsorbent for carbon dioxide and its kinetic studies. *Phys. E Low-Dimens. Syst. Nanostruct.* **2020**, *116*, 113739. [[CrossRef](#)]
102. Elsabay, K.M.; Fallatah, A.M. Fabrication of ultra-performance non-compact graphene/carbon hollow fibers/graphene stationary junction like membrane for CO₂-Capture. *Mater. Chem. Phys.* **2018**, *211*, 264–269. [[CrossRef](#)]
103. Sui, Z.Y.; Meng, Q.H.; Li, J.T.; Zhu, J.H.; Cui, Y.; Han, B.H. High surface area porous carbons produced by steam activation of graphene aerogels. *J. Mater. Chem. A* **2014**, *2*, 9891–9898. [[CrossRef](#)]
104. Nováček, M.; Jankovský, O.; Luxa, J.; Sedmidubský, D.; Pumera, M.; Fila, V.; Lhotka, M.; Klímová, K.; Matějková, S.; Sofer, Z. Tuning of graphene oxide composition by multiple oxidations for carbon dioxide storage and capture of toxic metals. *J. Mater. Chem. A* **2017**, *5*, 2739–2748. [[CrossRef](#)]
105. Varghese, A.M.; Reddy, K.S.K.; Singh, S.; Karanikolos, G.N. Performance enhancement of CO₂ capture adsorbents by UV treatment: The case of self-supported graphene oxide foam. *Chem. Eng. J.* **2020**, *386*, 124022. [[CrossRef](#)]
106. Shendell, D.G. Community outdoor air quality: Sources, exposure agents and health outcomes. *Encycl. Environ. Health* **2019**, 713–727. [[CrossRef](#)]
107. Vallero, D.A. Air pollution biogeochemistry. *Air Pollut. Calc.* **2019**, 175–206. [[CrossRef](#)]
108. Tabasum, A.; Alghuthaymi, M.; Qazi, U.Y.; Shahid, I.; Abbas, Q.; Javaid, R.; Nadeem, N.; Zahid, M. UV-accelerated photocatalytic degradation of pesticide over magnetite and cobalt ferrite decorated graphene oxide composite. *Plants* **2021**, *10*, 6. [[CrossRef](#)]
109. Mekonnen, M.M.; Hoekstra, A.Y. Sustainability: Four billion people facing severe water scarcity. *Sci. Adv.* **2016**, *2*, e1500323. [[CrossRef](#)] [[PubMed](#)]
110. Javaid, R.; Yaqub Qazi, U. Catalytic oxidation process for the degradation of synthetic dyes: An overview. *Int. J. Environ. Res. Public Health* **2019**, *16*, 2066. [[CrossRef](#)] [[PubMed](#)]

111. Rahman, M.U.; Qazi, U.Y.; Hussain, T.; Nadeem, N.; Zahid, M.; Bhatti, H.N.; Shahid, I. Solar driven photocatalytic degradation potential of novel graphitic carbon nitride based nano zero-valent iron doped bismuth ferrite ternary composite. *Opt. Mater.* **2021**, *120*, 111408. [CrossRef]
112. Masood, Z.; Ikhtlaq, A.; Akram, A.; Yaqub Qazi, U.; Shaheen Rizvi, O.; Javaid, R.; Alazmi, A.; Madkour, M.; Qi, F. Application of nanocatalysts in advanced oxidation processes for wastewater purification: Challenges and future prospects. *Catalysts* **2022**, *12*, 741. [CrossRef]
113. Ikhtlaq, A.; Javed, F.; Akram, A.; Qazi, U.Y.; Masood, Z.; Ahmed, T.; Arshad, Z.; Khalid, S.; Qi, F. Treatment of leachate through constructed wetlands using typha angustifolia in combination with catalytic ozonation on Fe-zeolite A. *Int. J. Phytoremediat.* **2020**, *23*, 809–817. [CrossRef]
114. Noureen, L.; Xie, Z.; Gao, Y.; Li, M.; Hussain, M.; Wang, K.; Zhang, L.; Zhu, J. Multifunctional Ag₃PO₄-rGO-Coated textiles for clean water production by solar-driven evaporation, photocatalysis, and disinfection. *ACS Appl. Mater. Interfaces* **2020**, *12*, 6343–6350. [CrossRef]
115. Nundy, S.; Ghosh, A.; Nath, R.; Paul, A.; Tahir, A.A.; Mallick, T.K. Reduced graphene oxide (rGO) aerogel: Efficient adsorbent for the elimination of antimony (III) and (V) from wastewater. *J. Hazard. Mater.* **2021**, *420*, 126554. [CrossRef]
116. Javaid, R.; Kawanami, H.; Chatterjee, M.; Ishizaka, T.; Suzuki, A.; Suzuki, T.M. Sonogashira C-C coupling reaction in water using tubular reactors with catalytic metal inner surface. *Chem. Eng. J.* **2011**, *167*, 431–435. [CrossRef]
117. Thakur, K.; Kandasubramanian, B. Graphene and graphene oxide-based composites for removal of organic pollutants: A review. *J. Chem. Eng. Data* **2019**, *64*, 833–867. [CrossRef]
118. Sun, H.; Liu, S.; Zhou, G.; Ang, H.M.; Tadó, M.O.; Wang, S. Reduced graphene oxide for catalytic oxidation of aqueous organic pollutants. *ACS Appl. Mater. Interfaces* **2012**, *4*, 5466–5471. [CrossRef]
119. Qazi, U.Y.; Iftikhar, R.; Ikhtlaq, A.; Riaz, I.; Jaleel, R.; Nusrat, R.; Javaid, R. Application of Fe-RGO for the removal of dyes by catalytic ozonation process. *Environ. Sci. Pollut. Res.* **2022**, *29*, 89485–89497. [CrossRef] [PubMed]
120. Dimitriou, P.; Javaid, R. A review of ammonia as a compression ignition engine fuel. *Int. J. Hydrogen Energy* **2020**, *45*, 7098–7118. [CrossRef]
121. Javaid, R. Catalytic hydrogen production, storage and application. *Catalysts* **2021**, *11*, 836. [CrossRef]
122. Cheng, J.; Zhang, M.; Wu, G.; Wang, X.; Zhou, J.; Cen, K. Photoelectrocatalytic reduction of CO₂ into chemicals using Pt-modified reduced graphene oxide combined with Pt-modified TiO₂ nanotubes. *Environ. Sci. Technol.* **2014**, *48*, 7076–7084. [CrossRef]
123. Quan, Q.; Xie, S.-J.; Wang, Y.; Xu, Y.-J. Photoelectrochemical reduction of CO₂ over graphene-based composites: basic principle, recent progress, and future perspective. *Acta Phys.-Chim. Sin.* **2017**, *33*, 2404–2423. [CrossRef]
124. Javaid, R.; Urata, K.; Furukawa, S.; Komatsu, T. Factors affecting coke formation on H-ZSM-5 in naphtha cracking. *Appl. Catal. A Gen.* **2015**, *491*, 100–105. [CrossRef]
125. Smallman, R.E.; Ngan, A.H.W. Physical properties. In *Modern Physical Metallurgy*; Elsevier: Amsterdam, The Netherlands, 2014; pp. 317–356. [CrossRef]
126. Gonzalez-Rodriguez, R.; Campbell, E.; Naumov, A. Multifunctional graphene oxide/iron oxide nanoparticles for magnetic targeted drug delivery dual magnetic resonance/fluorescence imaging and cancer sensing. *PLoS ONE* **2019**, *14*, e0217072. [CrossRef]
127. Zhang, M.; Cao, Y.; Chong, Y.; Ma, Y.; Zhang, H.; Deng, Z.; Hu, C.; Zhang, Z. Graphene oxide based theranostic platform for T₁-weighted magnetic resonance imaging and drug delivery. *ACS Appl. Mater. Interfaces* **2013**, *5*, 13325–13332. [CrossRef]
128. Chen, M.L.; Shen, L.M.; Chen, S.; Wang, H.; Chen, X.W.; Wang, J.H. In situ growth of β-FeOOH nanorods on graphene oxide with ultra-high relaxivity for in vivo magnetic resonance imaging and cancer therapy. *J. Mater. Chem. B* **2013**, *1*, 2582–2589. [CrossRef]
129. Enayati, M.; Nemati, A.; Zarrabi, A.; Shokrgozar, M.A. Reduced graphene oxide: An alternative for magnetic resonance imaging contrast agent. *Mater. Lett.* **2018**, *233*, 363–366. [CrossRef]
130. Khasraghi, S.S.; Shojaei, A.; Sundararaj, U. Highly biocompatible multifunctional hybrid nanoparticles based on Fe₃O₄ decorated nanodiamond with superior superparamagnetic behaviors and photoluminescent properties. *Mater. Sci. Eng. C* **2020**, *114*, 110993. [CrossRef]
131. MRI Basics. Available online: <https://case.edu/med/neurology/NR/MRIBasics.htm> (accessed on 5 January 2023).
132. Alazmi, A.; Singaravelu, V.; Batra, N.M.; Smajic, J.; Alyami, M.; Khashab, N.M.; Costa, P.M.F.J. Cobalt ferrite supported on reduced graphene oxide as a T₂ contrast agent for magnetic resonance imaging. *RSC Adv.* **2019**, *9*, 6299–6309. [CrossRef] [PubMed]
133. Mohanta, Z.; Gaonkar, S.K.; Kumar, M.; Saini, J.; Tiwari, V.; Srivastava, C.; Atreya, H.S. Influence of oxidation degree of graphene oxide on its nuclear relaxivity and contrast in MRI. *ACS Omega* **2020**, *5*, 22131–22139. [CrossRef] [PubMed]
134. Peng, S.; Feng, P.; Wu, P.; Huang, W.; Yang, Y.; Guo, W.; Gao, C.; Shuai, C. Graphene oxide as an interface phase between polyetheretherketone and hydroxyapatite for tissue engineering scaffolds. *Sci. Rep.* **2017**, *7*, srep46604. [CrossRef]
135. Bin Jo, S.; Erdenebileg, U.; Dashnyam, K.; Jin, G.-Z.; Cha, J.-R.; El-Fiqi, A.; Knowles, J.C.; Patel, K.D.; Lee, H.-H.; Lee, J.-H.; et al. Nano-graphene oxide/polyurethane nanofibers: Mechanically flexible and myogenic stimulating matrix for skeletal tissue engineering. *J. Tissue Eng.* **2020**, *11*, 2041731419900424. [CrossRef]
136. Sun, X.; Liu, Z.; Welsher, K.; Robinson, J.T.; Goodwin, A.; Zaric, S.; Dai, H. Nano-graphene oxide for cellular imaging and drug delivery. *Nano Res.* **2008**, *1*, 203–212. [CrossRef] [PubMed]
137. Karki, N.; Tiwari, H.; Tewari, C.; Rana, A.; Pandey, N.; Basak, S.; Sahoo, N.G. Functionalized graphene oxide as a vehicle for targeted drug delivery and bioimaging applications. *J. Mater. Chem. B* **2020**, *8*, 8116–8148. [CrossRef] [PubMed]

138. Xiao, Y.; Zhang, M.; Fan, Y.; Zhang, Q.; Wang, Y.; Yuan, W.; Zhou, N.; Che, J. Novel controlled drug release system engineered with inclusion complexes based on carboxylic graphene. *Colloids Surf. B Biointerfaces* **2019**, *175*, 18–25. [[CrossRef](#)]
139. Deb, A.; Vimala, R. Natural and synthetic polymer for graphene oxide mediated anticancer drug delivery—A comparative study. *Int. J. Biol. Macromol.* **2018**, *107*, 2320–2333. [[CrossRef](#)]
140. Lin, J.; Chen, X.; Huang, P. Graphene-based nanomaterials for bioimaging. *Adv. Drug Deliv. Rev.* **2016**, *105*, 242–254. [[CrossRef](#)]
141. Kurniawan, A.; Muneekaew, S.; Hung, C.W.; Chou, S.H.; Wang, M.J. Modulated transdermal delivery of nonsteroidal anti-inflammatory drug by macroporous poly(vinyl alcohol)-graphene oxide nanocomposite films. *Int. J. Pharm.* **2019**, *566*, 708–716. [[CrossRef](#)] [[PubMed](#)]
142. Chen, Y.; Yang, Y.; Xian, Y.; Singh, P.; Feng, J.; Cui, S.; Carrier, A.; Oakes, K.; Luan, T.; Zhang, X. Multifunctional graphene-oxide-reinforced dissolvable polymeric microneedles for transdermal drug delivery. *ACS Appl. Mater. Interfaces* **2020**, *12*, 352–360. [[CrossRef](#)] [[PubMed](#)]
143. Li, J.; Zeng, H.; Zeng, Z.; Zeng, Y.; Xie, T. Promising graphene-based nanomaterials and their biomedical applications and potential risks: A comprehensive review. *ChemMedChem* **2022**, *17*, e202200142. [[CrossRef](#)]
144. Diez-Pascual, A.M.; Rahdar, A. Functional Nanomaterials in Biomedicine: Current Uses and Potential Applications. *J. Am. Chem. Soc.* **2008**, *130*, 10876–10877. [[CrossRef](#)]
145. Shen, H.; Zhang, L.; Liu, M.; Zhang, Z. Biomedical applications of graphene. *Theranostics* **2012**, *2*, 283–294. [[CrossRef](#)] [[PubMed](#)]
146. Quagliarini, E.; Di Santo, R.; Pozzi, D.; Tentori, P.; Cardarelli, E.; Caracciolo, G. Mechanistic Insights into the release of doxorubicin from graphene oxide in cancer cells. *Nanomaterials* **2020**, *10*, 1482. [[CrossRef](#)]

Disclaimer/Publisher’s Note: The statements, opinions and data contained in all publications are solely those of the individual author(s) and contributor(s) and not of MDPI and/or the editor(s). MDPI and/or the editor(s) disclaim responsibility for any injury to people or property resulting from any ideas, methods, instructions or products referred to in the content.